Graded magnetic materials

Lorenzo Fallarino[1], Brian J. Kirby[2], and Eric E. Fullerton[3,4]

[1]CIC Nanogune BRTA, E-20018 Donostia - SanSebastian, Spain.

[2]NIST Center for Neutron Research, Gaithersburg, Maryland 20899, USA

[3]Center for Memory and Recording Research, University of California, San Diego, La Jolla, California, 92093-0401, USA

[4]Department of Electrical and Computer Engineering, University of California, San Diego, 9500 Gilman Drive, La Jolla, California 92093-0407, USA

Abstract

Graded magnetic materials represent a promising new avenue in modern material science from both fundamental and application points of view. Over the course of the last few years, remarkable results have been obtained in (epitaxial) heterostructures based on thin alloy films featuring diverse compositional depth profiles. As a result of the precise tailoring of such profiles, the exchange coupling, and the corresponding effective or local Curie temperatures can be controlled over tens of nm with an excellent precision. This topical review article reports the most recent advances in this emerging research field. Several aspects are covered, but the primary focus lies in the study of compositional gradients being transferred into depth dependent magnetic states in ferromagnets, while also reviewing other experimental attempts to create exchange graded films and materials in general. We account for the remarkable progress achieved in each sample and composition geometry by reporting the recent developments and by discussing the research highlights obtained by several groups. Finally, we conclude the review article with an outlook on future challenges in this field.

1. Introduction

Thin film systems exhibiting spatially dependent magnetic properties merged as an exciting research field showing promise for improving performances of many technological applications [1-7]. It is interesting to realize that the idea of structures with graded properties has its origin in nature, where they are commonly found as bones, teeth, skin, biological tissues, or plants [8-12]. While being artificially brought to far smaller length scales, such spatial nonuniformities were initially generated via self-assembly or segregation dynamics rather than by direct manufacturing design, providing a modest but sufficient level of control of the spatial variation of densities or compositions [13-16].

A qualitative step forward became possible via the growth of materials that exhibit (sub) nm-scale depth-dependent profiles [17-20], which allowed for the creation of exact growth profiles along the thickness direction and not relying on segregation and phase separation. Such a depth-dependent grading concept was originally utilized in magnetic structures made of very sharp layering, for example in ferromagnetic / non-magnetic / ferromagnetic (FM/NM/FM) trilayers, a material system that led to one of the more fascinating and impactful advances in solid state physics, the discovery of giant magneto-resistance (GMR) [21,22]. GMR involves regions of device with tuneable relative directions of magnetization creating major differences in electrical resistance. It has had a tremendous impact on electronics, especially read heads in hard disk drives (HDD), where magnetically stored information can be read efficiently through distinct electrical signals [21-24]. Thanks to GMR and layer tunnelling magnetoresistance (TMR) [25], high capacity HDD are possible today [26,27].

Hereby, significant advances have emerged from layered structured with sharp interfaces as discussed in detail in [28]. In most cases, the new physics and functionality arise from the discrete boundaries between disparate materials such as in the case of GMR or as in artificial FM/ heavy-metal multilayers [29-34] that are known to exhibit an out-of-plane easy magnetization axis due to their strong interfacial anisotropy. As such, another example are metamagnetic/ferromagnetic bilayer structures [35-40], which can exhibit a very steep temperature (T) dependence of the magnetic coercivity (H_C), promoting them as good candidates for applications as recording media for heat assisted magnetic recording (HAMR) [41,42]. However, researchers have yet to find pathways to broadly tune the associated thermally activated transitions and by doing so achieve technological relevance. Moreover, such systems may be challenged by structures that naturally exhibit depth-dependent FM / antiferromagnetic (AFM) interfaces leading to extremely large dH_C/dT gradients [43-46].

However, class of heterogeneous material where the properties (e.g. composition, Curie temperature, magnetization) vary more gradually, which we refer to as graded materials, is the focus of this review.

Here, we aim to report the state-of-the art of graded magnetic materials research field. The review begins by informing the reader within their historical technological evolution starting by exchange spring systems, which consist of anisotropic hard/soft ferromagnetic bilayers (Section 2). In Section 3 we focus on the closest precursor of exchange graded structures, which are multilayers where the magnetic anisotropy increases from layer to layer or even continuously. The fourth Section opens with the experimental evidence of NiCu linear exchange graded films exhibiting a ferromagnetic phase transition similar to what one would expect from a continuum of uncoupled ferromagnetic layers with distinct local Curie temperatures. Section 5 continues with the temperature decorrelation in NiCu graded interlayers and in epitaxial CoCr graded films. However, over short enough distances, a ferromagnetic system cannot be local and interlayer exchange coupling must start to dominate. Section 6 and Section 7 covers exactly this aspect, understanding the localization limit and its relevancy for applications in amorphous (Section 6) and single crystal (Section 7) graded structures. This Section will also review experimental characterization methods to confirm the material grading. Section 5 and 7 provides also examples of convenient material types that can be grown epitaxially with uniaxial magnetocrystalline anisotropy in the film plane to achieve negligible in-plane demagnetization fields and thusly perform detailed and quantitative analysis. The eighth and final Section is dedicated to exploring the practical consequences of the above described findings, providing guidance to materials design for applications.

2. Exchange Spring Media

As already introduced, the depth-dependent grading concept was primarily employed in magnetic systems that were consisting of abrupt layering. In this context, an interesting material-type structure are exchange-spring ferromagnets, which are systems that are formed by soft and hard magnetic layers (or phases) that are exchange-coupled at their interface [47]. Figs. 1(a) and 1(b) show a simplified depth profile of the relevant magnetic properties, changing abruptly at the interface between the two layers. This thin-film sample architecture was firstly devised by Goto et al. already in 1965 [48] and then proposed in 1991 by Kneller and Hawig [5] for application in permanent magnet. The coupled bilayer configuration led to an enhanced (B·H) energy product especially if compared to the values of the constituting phases [6,49,50]. In fact, this approach offered several potential advantages over the

conventional development of single high-anisotropy materials with high saturation magnetization M_S and Curie temperature T_C [51,52], since the spatial anisotropy variation becomes the relevant tuning parameter. Moreover, exchange-spring ferromagnets have the additional benefit of reducing the rare-earth content when the hard phase is a rare-earth transition-metal phase. In the past years, numerous scientific investigations have been instrumental for the derivation of optimized parameters of the magnetically soft and hard regions [53-56], by using a material approach in which different model systems were investigated in terms of detailed structural and magnetic characterizations [57-59]. In addition, the optimum interface structure is being explored and it was found that a graded interface between the hard and soft layer can further enhance the properties [60].

Exchange-spring ferromagnets have also become important test systems for the study of non-collinear magnetism, since the application of a magnetic field of sufficient strength could lead to the formation of non-collinear spiral-like structure in the soft magnetic material, as depicted in Fig. 1(c) [61,62]. Indeed, based on this reversible rotation of the magnetic moments of the soft layer, Kneller and Hawig created the “exchange spring” term in analogy with the mechanics of a spring [5].

The associated magnetization reversal curve of an exchange-spring magnet is schematically depicted in Fig. 1(d). In the high field regime, the system exhibits, throughout the entire bilayer, a uniform magnetization state parallel to the field direction and so it behaves as a single-phase material. Once the external magnetic field is reversed, the saturated state becomes unstable at a magnetic field denoted as H_{ex} and undergoes vertically magnetization rotations, which culminates in the formation of a spiral-like magnetic structures in the soft phase [63,64]. As the reverse field strength increases, compresses at the interface, and finally triggers the magnetization reversal of the hard magnetic material. The latter process starts rather abruptly at the irreversible field H_{irr}, leading to a drop in the magnetization that is highlighted in red in Fig. 1(d). Therefore, the $M(H)$ curve for bilayer spring magnets contain two characteristic transitions [7], which are very different in their nature. Since the soft and hard phases are only exchange coupled at the interface, the reorientation of the soft layer is fully reversible between $H_{ex} < H < H_{irr}$, undergoing a second-order phase transition, whereas the magnetization of the hard layer changes its direction irreversibly, and it occurs as a first-order phase transition.

Both the corresponding theoretical description and further experimental realization of exchange spring magnets provided a convenient model system for developing precise spatial control of the magnetic properties in multilayer systems, resulting in the tailor of the hysteresis

loop characteristics in a wide range by for instance controlling the relative thickness of the magnetically hard and soft layers [35, 65-68]. In fact, by increasing (decreasing) the thickness of the soft (hard) layer, the magnetization reversal curve of the bilayer system would become typical of two independent layers material, as the two sample regions would magnetically reverse independently and irreversibly at different magnetic fields. Further interest in this multilayer stacking approach were driven by the proposal of exploiting magnetic anisotropy graded materials, supported by theoretical predictions that they could prove advantageous for data storage technology [20,69-75]. In the following Section we will focus on this specific material type structures.

3. Graded anisotropy spring media

More recently, an innovation that goes beyond bilayer systems is the concept of continuously varying the magnetic anisotropy along the growth direction or thickness *z*. Such pre-designed depth dependent structures aimed to achieve a field driven magnetization reversal state that is non-collinear in its nature [73-75], and so overcoming a major technological problem [15]. The switching field can indeed potentially be decreased to an arbitrarily small value while keeping the energy barrier constant to thermal reversal sufficiently high [73], thus allowing writability and thermal stability to be separately optimized. Specifically, anisotropy depth profiles that decreases as a function of $1/z^2$ theoretically provide the largest switching field reduction, especially once compared to layered materials with similar thermal stability values. As such, anisotropy graded materials, which can be considered as a progression of exchange spring media, are a recent technologically relevant example, for which a very specific smoothly graded structure was proposed and utilized as HDD applications.

The basic principle of graded anisotropy spring media is illustrated in Fig. 2. Under zero applied magnetic field, two stable states with equal energy exist corresponding to opposite magnetization orientation. By assuming one of the two as the initial equilibrium direction for the magnetization, the reversal occurs when the local minimum at which the system is initially placed becomes a saddle point. This happens by applying a magnetic field opposite to the initial magnetization orientation, which reduces the barrier separating the metastable state and the stable state to zero, upon which the magnetization ‘jumps’ to the new state via a switching mechanism. In graded anisotropy spring media, due to the introduction of magnetic layers with different magnetic anisotropy constants, the slope of the energy landscape decreases, as depicted on the bottom right side of Fig. 2. Consequently, the energy landscape gets stretched in the horizontal direction, while the thermal barrier remains mostly unaltered, and therefore

the required magnetic field strength to switch the magnetic state can be reduced and designed to match the technological needs. As such, graded anisotropy spring materials are a recent technologically relevant example of depth-dependent grading concept, for which a very specific smoothly magnetic anisotropy structure was proposed and utilized. Stimulated by these promising results, numerous research groups have been successful in fabricating graded anisotropy media, including exploiting different growth temperatures [76-79], post-growth annealing and diffusion [80-83], different working gas pressures [84], composition gradients [85-88], modulated layer thickness in multilayers [20,89], ion irradiation effects in soft/hard bilayers [90,91] and ion implantation of specific ions [92]. Some of these fabrication procedures are indeed rather complex and, because of their complexity, these graded anisotropy materials have not, as yet, achieved significant technological relevance.

Nevertheless, the successful creation of vertically graded anisotropy profiles provided remarkable insights towards unveiling novel functionalities associated with the spatial control of the modified energetic terms in such systems.

4. Exchange graded structures

More recent studies have demonstrated that not only magnetic anisotropy gradients can be realized and explored along the thickness, but that it is also possible to achieve continuous modification of the exchange coupling constant (J) parallel to the growth direction. Marcellini et al. [18] took advantage of finite size effects in high quality Fe(001)/V(001) multilayers to design nanoscale modification of J. The Fe layers had distinct effective T_C due to the different thicknesses ranging from 2 to 3 monolayers, whereas the thickness of the V interlayers was kept constant to ensure fixed magnitude and sign of the interlayer coupling. The influence of the T_C distribution triggered unexpected temperature dependence of the magnetization of such coupled layered magnets, suggesting the presence of a vertically moveable quasi-phase boundary dividing FM from paramagnetic (PM) regions [18].

A qualitative step forward from this layered graded materials design was made by LeGraët et al. [93], which explored materials that are derived from smoothly changing the chemical doping density during growth, similarly that in graded seed layers, where the composition was gradually changed to relieve strain and lattice mismatch for the epitaxial growth of relaxed and low-dislocation-density layers [94-96]. Ref. 93 demonstrated the feasibility of a movable AFM - FM phase boundary in Ir- and Pd- doped FeRh films [93]. Such horizontal AFM-FM “domain-wall” could move gradually in position throughout the layer by increasing or decreasing the temperature, affecting the magnetisation and electric resistivity of

the compositional-graded FeRh layer to be controlled and exploited for novel device applications [93].

This quasi-phase boundary mobility was deeper investigated in linear doping profiles to yield fine control over the FM - PM phase transition in terms of both temperatures ranges and space distribution [97]. In Ref. 97 a (111) textured $Ni_{x(z)}Cu_{1-x(z)}$ thin alloy film with a linear variation of the Cu dopant concentration along the thickness was studied as a model system. Hereby, it is important to remind that the T_C can be tuned by alloying the FM with a NM material [98,99], which is typically related to the increase of the NM material in the alloy. By inducing systematic variations in composition, as performed in Ref. 97, it was possible to achieve and tailor the NiCu alloy system to exhibit a predefined depth dependent J profile along the growth direction, as depicted in Fig. 3(a). More importantly, this showed that such nanoscale materials behave as composed of virtually independent ferromagnetic (sub-)layers, so that each local J value generates a "local" Curie temperature ($\tilde{T}_C$) [97], despite, from a thermodynamic perspective, a ferromagnetic material should exhibit only one single T_C [100,101]. The type of sample of Ref. 97 allowed moreover to map the temperature-dependent ferromagnetic state onto a depth-dependent spatial profile, as shown in Fig. 3(b) and 3(c), which was confirmed both experimentally and theoretically [97]. As a consequence of such acquired spatial nature of the ferromagnetic state, a quasi-phase boundary emerges separating ordered from disordered magnetic regions within the same ferromagnetic sample, which can be altered controllably and reversibly by temperature [97].

5. Thermomagnetic switch via graded interlayer exchange coupling

Interlayer exchange coupling (IEC) is one of the key fundamental characteristics of artificially layered systems [102,103], important for applications in information processing and storage [104]. In many cases it influences the magnetic order and the magnetization switching under externally applied fields [105] or spin-polarized currents [106-108]. The IEC is oscillatory as a function of the NM spacer thickness [109-111], and it can be varied between antiferromagnetic and ferromagnetic-like coupling type, while being fixed during fabrication by selecting a specific NM spacer thickness [112]. For instance, once the coupling is set to be antiferromagnetic, an external magnetic field is necessary to change the state of the structure to be parallel. It would be highly desirable to devise a material where the IEC could gain controllability by varying an external physical parameter. Anderson and Korenivski [113,114] devised a system made of strong / weak / strong ferromagnetic trilayer (hereinafter FM/fm/FM), where the fm spacer has a lower T_C than the FM outer layers. By heating such

trilayer structure above the T_C (fm), the outer FM layers can be exchange-decoupled, so that their parallel alignment below T_C (fm) can be switched to antiparallel above T_C (fm) in a reversible way. This material concept opened new perspectives for the thermal control of the IEC, for instance by resistive heating generated by an electric current [113,114].

Kravets et al. [115] made significant progress in this field by replacing the homogenous fm interlayer by an exchange coupling strength graded spacer. The corresponding sample structure is illustrated in Fig. 4(a), consisting of a Py layer that is exchanged bias by an AFM $Ir_{20}Mn_{80}$ layer, of a $Ni_{x(z)}Cu_{1-x(z)}$ graded spacer, and of a second Py layer on top, resulting in asymmetric AFM/FM/graded-spacer/FM system. The *J* profile of the spacer is depicted in the same Fig. 4(a) as red line, which follows a bathtub-like structures. Such profile was proposed to minimize the ferromagnetic proximity effect at the FM/graded-spacer interfaces by means of the reduced Ni concentration at such interfaces, and consequently improving the thermal control of the switching behaviour of the multilayer material [115,116]. The so-called thermomagnetic switching was demonstrated by following a specific measurement procedure in Ref. [115] (i) the samples were first heated just above the critical temperature of the central region of the graded spacer material T_C*, but below any significant thermally induced reduction of the exchange bias (ii) a magnetic field was applied in the film plane opposite to the pinning direction (iii) the temperature was gradually decreased down to room temperature (RT) while measuring the in-plane magnetization amplitude. It is important to highlight that the central region of the $Ni_{x(z)}Cu_{1-x(z)}$ spacer, while crossing its T_C^* during cooling, undergoes its PM - FM phase transition, as depicted in Fig. 4(b). As a result, the spacer acts as an exchange spring of increasing strength, which rotates the free Py layer during the cooling from being along the bias field toward the pinning direction. Such thermomagnetic switching demonstrated in Ref. [115,116] offers the significant advantage of highly tuneable T_C^*, which is not linked to the Néel temperature T_N of the AFM [117]. Furthermore, the FM-PM transition is typically fully reversible and therefore does not suffer from training-like effects typical of exchange-biased FM/AFM interfaces [118].

This route to novel materials design was taken further with the accomplishment of continuous compositional gradients being transferred into depth-dependent magnetic states in single layer ferromagnets [119]. The key goal was to investigate whether a $\tilde{T}_C$ depth profiles, as the one of Ref. 97, could be utilized to modify the magnetization reversal within one single ferromagnetic graded material. Ref. 119 selected CoCr alloys as test material, since the corresponding magnetic properties can be easily tuned by changing the Cr doping concentration [120,121]. Moreover, the alloy forms a stable solid solution in a wide Cr range

while preserving the original hcp crystal structure of pure Co to make magnetostatic energy irrelevant [98]. It was devised and studied a series of epitaxial symmetric graded CoCr samples, whose layer growth sequence is shown in Figure 5(a), with the maximum Cr content x_c (with x_c ranging from 0.25 to 0.32) at the centre of the graded structure, as depicted in Fig. 5(b). The magnetometry characterization revealed a temperature- and composition-dependent magnetization reversal process, with a fully correlated magnetic structure with one step switching behaviour for temperatures below the $\tilde{T}_C(x_c)$ of the central high Cr doping region, whereas a two-step switching above this temperature.

As an example, in the following we discuss in detail the results obtained for the sample with x_c = 0.28. Cu-K_α x-ray diffraction measurements, shown in Fig. 5(c), confirmed the epitaxial growth quality [98,119], corroborated by the absence of signals corresponding to non-epitaxial crystal orientations and thus demonstrating the excellent crystallographic order [98,119]. The in-plane uniaxial magnetocrystalline anisotropy behaviour was verified by Vibrating Sample Magnetometer (VSM) measurements. Specifically, RT magnetization reversals were measured for various orientations of the in-plane applied magnetic field β with respect to the c-axis [98,119]. The results are displayed in Figure 5(d) as color-coded magnetization maps, which confirm the uniaxial magnetic anisotropy with the c-axis being the preferential magnetization axis. This was further corroborated by the good agreement between the measurement and the least-squares fit [Fig. 5(e)], which was performed by using a simple macrospin model [98]. The combination of VSM and MOKE experimental techniques [119], shown in Fig. 5(f), allowed to determine that the sample is not anymore magnetically correlated throughout the entire thickness at room temperature, due to the magnetic phase change of the central $Co_{1-x(z)}Cr_{x(z)}$ layer [119], resembling a system made up of two exchange decoupled magnetic layers with distinct switching fields [122]. To better visualize these experimental data and especially the different switching regimes, Figure 5(g) show as color-coded maps the normalized magnetization M/M_S as a function of temperature and the reduced field h = (H-$\overline{H}_S$)/ $\overline{H}_S$, with $\overline{H}_S$ being the average of the two switching fields: for T > 260 K the reversal occurs in two steps, indicated by the triangular-shaped (green) area, whereas for T < 260 K a single step switching is observed, in very good agreement with the transition temperature of x = 0.28 uniform alloys [123].

The direct measurement of such temperature dependent decorrelation was performed by polarized neutron reflectometry (PNR) [119], whose results are summarized in Figures 5(k) and 5(l). PNR unambiguously demonstrated that the x_c = 0.28 graded sample promotes a

transition from one-step to two-step reversal behaviour for temperatures T > 260 K, indicating a transition from a fully correlated magnetic film structure to an uncoupled system containing effectively two independent magnetic sublayers. Therefore, rationally designed composition profiles can be envisioned to achieve desired temperature and field dependencies by facilitating collective or noncollective magnetic behaviour [119].

6. Magnetic proximity effects in amorphous *J* graded systems

Having established in Section 4 the existence of internal quasi-phase boundaries separating ordered from disordered magnetic regions within the same ferromagnetic graded sample, it became important to evaluate whether such FM-PM interfaces may be atomically sharp or instead exhibit a specific extension. Indeed, in general, at the interface formed by a magnetic and non-magnetic material, the magnetic order can drastically influence the properties of the non-magnetic component [124-126]. It is typically observed in layered structures, where one component is FM or AFM and the other is PM or has a lower ordering temperature [127]. In FM-PM systems a magnetization can be induced in the PM material and in FM-FM or FM-AFM systems the critical temperature (T_C or T_N) can be modified [128-130]. The induced magnetization can in turn result in non-oscillatory interlayer exchange coupling across metallic spacers [131] as well as spring-magnetic behaviour and long range exchange bias through paramagnetic layers [129].

This proximity effect is usually short-ranged [126,127,132]. For example, in Fe/V multilayer systems the magnetic moment in the V has an exponential decay length of approximately 0.3 nm [132] but by replacing the V with FeV the decay length could be extended to 1.7 nm [133]. A larger proximity effect can be achieved in high susceptibility paramagnets such as Pd and Pt, where the induced magnetization can extend up to a few nm [134-136]. However, Ref. 128 has shown that in amorphous heterostructures the effect can extend to several tens of nm into the nonmagnetic material. This is achieved by tuning the composition of the amorphous alloys such that the T_C can be easily controlled without significantly affecting the interface structure [137]. In addition, the material density modulations in such disordered alloys could contribute to enlarge the proximity effect extension [138].

Following the previous findings, K. A. Thórarinsdóttir et al. [139] explored amorphous multilayers that are composed of alternating high- and low- *J* (T_C) materials by a combination of magnetometry and PNR. The investigated samples structure is schematically shown in Fig. 6(a), consisting of a 2-nm thick $Al_{70}Zr_{30}$ buffer layer, a multilayer made of $[Co_{85}(Al_{70}Zr_{30})_{15}$ (1

nm) / $Co_{60}(Al_{70}Zr_{30})_{40}$ (5 nm)]$_N$, and a 3-nm thick $Al_{70}Zr_{30}$ capping layer. The RT growth, choice of compositions, and the use of an $Al_{70}Zr_{30}$ buffer layer ensured sharp interfaces and amorphous films [140,141]. The corresponding exchange depth profile is depicted in Fig. 6(b), with a low value of J corresponding to the $Co_{60}(Al_{70}Zr_{30})_{40}$ layers and the high J value to $Co_{85}(Al_{70}Zr_{30})_{15}$ layers. If grown separately, the difference in Co content would result in different T_C of the two stoichiometries. In fact, the $Co_{85}(Al_{70}Zr_{30})_{15}$ has an ordering temperature that is well above RT, whereas $Co_{60}(Al_{70}Zr_{30})_{40}$ has a far smaller T_C as shown by the illustration in Fig. 6(c). Below their ordering temperatures, both systems are ferromagnetic with the magnetization of the layer $Co_{60}(Al_{70}Zr_{30})_{40}$ being significantly lower than that of $Co_{85}(Al_{70}Zr_{30})_{15}$ in a significant temperature range. However, once the two different AlZr doped Co layers are grown amorphously in a multilayer form, Thórarinsdóttir et al. [139] demonstrated that, for temperatures between the two ordering temperatures, proximity effects can induce an almost constant magnetization with a remarkably long extension in the $Co_{60}(Al_{70}Zr_{30})_{40}$ paramagnetic material. PNR measurements showed the presence of an interface region of smoothly varying magnetization between the individual layers, with the ordering temperature of the 5 nm thick $Co_{60}(Al_{70}Zr_{30})_{40}$ layers being enhanced. Above such temperature, a magnetically ordered state with a very large extension was observed in the multilayer paramagnetic regions. The amorphous nature of the multilayer structure and the selected composition range of the films were proposed to explain this large extension of the proximity effect through the 5 nm thick $Co_{60}(Al_{70}Zr_{30})_{40}$ [142]. In fact, the inherent local variation in the concentration of the magnetic element within the amorphous alloy means that it will inevitably have local variations in T_C with interconnected regions of high and low magnetic coupling strength [143].

These results demonstrate the complexity of magnetic proximity effects in amorphous metals and how they can fundamentally alter the behaviour of such materials in layered structures. Much is still unknown about the nature of the induced magnetization and the potential for controlling its size and extension with parameters other than temperature. Indeed, magnetic proximity effects must be considered in the design of magnetic structures at the nanoscale. For example, we have shown in Section 4 that systematic variation of the exchange coupling strength can be used to create systems that exhibit “local” Curie temperatures. Such localization of thermodynamic behaviour is however largely dependent on the inherent spatial resolution of magnetic properties. Specifically, over short enough distances, interlayer exchange coupling must start to dominate the effects of the compositional gradient.

Understanding this localization limit is important for potential applications, as it dictates the length scale, below which graded material design stops being feasible.

7. Magnetic localization limit in *J* modulated single crystal ferromagnets

Although Ref. [97] demonstrated that the local Curie temperature $\tilde{T}_C$ of a graded structure can be continuously varied via compositional gradients over tens of nm, over very short distances an itinerant ferromagnetic system should not exhibit in principle purely local properties and the exchange coupling along the *z*-axis should start to dominate the effects of any compositional gradient. To study this limit, Ref. 144 has employed CoRu alloy structures, specifically an oscillatory compositional depth profile produced by a "triangular" Ru content profile exploring different oscillation periods λ. By changing λ, the authors aimed to explore the lowest limit of transferring compositional effects into modulated magnetic states. The Ru concentration x was linearly decreased from 0.31 to 0.21, and subsequently increased linearly back to 0.31 in each period. A series of such "triangular" graded $Co_{1-x(z)}Ru_{x(z)}$ epitaxial thin films were grown on top of a Si/Ag/Cr/CrRu layer sequence with λ = 10 and 20 nm [Figure 7(a)] [98,145]. CoRu alloy was selected for this study as it is a very simple ferromagnet with easily tuneable magnetic properties [98,146-149]. Further, CoRu can be grown with the hcp crystal structure and $(10\bar{1}0)$ orientation to have an in-plane easy axis [98,99,150-152]. CoRu was also chosen because Ru brings contrast advantages for subsequent PNR measurements [153].

Cu Kα x-ray diffraction measurements confirmed the epitaxial growth quality, as shown in Fig. 7(b), demonstrating excellent crystallographic order. Figure 7(c) and 7(d) display as color-coded maps the RT normalized magnetization M/M_S data as a function of the magnetic field strength $\mu_0 H$ and the field angle β for both λ = 10 nm (c) and 20 nm (d). These data sets were assembled as described in Ref. 144. Both experimental maps indicate that the samples exhibit uniaxial in-plane anisotropy with the easy axis coinciding with the c-axis, corroborated by the excellent agreement with the least-squares fits to a macrospin model [98] of Figure 7(e) and 7(f). The temperature-dependent easy-axis magnetizations $M(T)$ were measured in a 5 mT in-plane field and are shown in Fig. 7(g), together with the $M(T)$ curves of homogenous reference $Co_{0.69}Ru_{0.31}$ and $Co_{0.71}Ru_{0.21}$ samples. The uniform x = 0.21 sample exhibits a much larger T_C than the uniform x = 0.31 sample, with the modulated λ = 10 nm and λ = 5 nm curves falling in between. Values of T_C [154] were estimated T_C = 230 K for x = 0.31 and T_C = 560 K for x = 0.21 [144], generally consistent with Ref. 98. The magnetic modulation of the λ = 10 nm and λ = 5 nm samples was confirmed by PNR [144]. Figures 8(a) and 8(c) display the R^{++}

and R^{--} reflectivities for the λ = 10 nm (a) and λ = 5 nm (c) both measured at T = 50 K. The data exhibit pronounced spin-dependent oscillations as a function of Q together with the multilayer Bragg peaks near Q = π / λ, marked by black arrows, indicating the high degree of coherence in the structural and magnetic layering. Very good agreement was found between the data and the fit, which yielded the nuclear scattering depth profile ρ_N and magnetic depth profile that are shown in Figures 8(b) and 8(d) as black and red lines respectively [144]. Therefore, PNR verified that continuous compositional gradients can be used to generate continuous magnetic modulation profiles even on length scales very close to the ferromagnetic exchange length.

To compare the experimental results with theoretical expectations, the magnetization modulation was calculated, following a previous work [97], for a model system that mimics the experimental one in the framework of the mean-field approximation (MFA) of the Ising model [144]. Figure 8(e) depicts the unit cell used for calculations, while the intrinsic modelled exchange strength profile is shown in Fig. 8(f), which features the triangular exchange profile of the samples. In Ref. 144 it was conveniently defined the normalized local Curie temperature modulation $\Delta t_C = T_C^{max} - T_C^{min} / T_C^{max}$ as a figure of merit for quantitatively describing variation in T_C, and an exchange delocalization distance in absolute units, $d_{dl} = 2Nd_{\beta}$, where N is half the number of layers over which the exchange interaction is extended. Figure 8(g) shows the MFA calculated Δt_C for λ = 5 nm (orange lines) and λ = 10 nm (blue lines). As d_{dl} approaches zero, the individual layers become progressively more isolated, and Δt_C for both λ converge to the value expected for the uniform reference samples (Δt_C = 0.59 [144]). As the delocalization distance d_{dl} increases, the layers become increasingly more coupled, the magnetization profiles become more homogeneous, and Δt_C approaches zero. Experimental values of Δt_C as determined from PNR are depicted as open symbols in Fig. 8(g) [144], and notably, they intersect the horizontal axis at nearly the same value of d_{dl} for both λ. Yellow shading in Fig. 8(g) indicates the range of possible values of d_{dl} based on the model of Ref. 144 and fitting uncertainty, demonstrating that the delocalization distance is less than approximately 3 nm and may be less than 1 nm if the samples are indeed more locally perfect than they appear to PNR, smaller than the magnetostatic exchange length for pure Co $l_{ex} \approx 4$ nm [155].

Therefore, the work presented in Ref. 144 has shown that for virtually any modulated ferromagnetic system, nonlocal materials properties are likely insignificant over length scales greater than ≈ 3 nm, where the thermodynamic behaviour can be described in terms of local

properties. [144,150]. In addition to being fundamentally interesting, this degree of localization has important implications for devices and materials development [156].

8. Conclusions and Outlook

This review highlights the still emerging graded magnetic material research field, describing its development from the first attempts to verify the functional concept in exchange spring magnet [5] to the realization of continuous composition gradients that translates into continuous local Curie temperature gradients at the nm length scales [144,150]. The developed material platform and related findings have practical consequences by demonstrating that down to few nanometres [144], many aspects of magnetic properties can be predicted by using a local picture, including a local T_C description. Despite such outstanding progress, many questions remain unanswered. For instance, the role of the internal PM-FM quasi-phase boundaries, that are expected to be increasingly important when reducing film thickness, requires the joint action of thin film preparation, exhaustive magnetic characterization, and theoretical modelling to delineate its impact into the critical behaviour close to T_C.

On the other hand, most of the work has been carried out on graded magnetic systems that were grown on ideally flat substrates, and as a result the demagnetizing fields are strongly suppressed in the surface of the film. However, in the case of ferromagnetic films with a given anisotropic roughness in the surface, the demagnetizing fields could lead to an additional magnetic anisotropy that depends on the surface patterning [157]. One could envision to fabricate graded magnetic films with tuneable anisotropy, that might acquire a depth dependent profile and could have potential applications in spin-logic circuits and/or spin ice systems.

Actually, the competition between perpendicular magnetic anisotropy (favouring a perpendicular magnetisation state) and demagnetizing fields (favouring an in-plane magnetisation state) is the responsible of the magnetic reorientation transition in thin magnetic films [158]. In graded magnetic materials, though, the actual ferromagnetic film thickness can be varied with temperature within one single sample and consequently the demagnetizing fields can be actively modified. Therefore, graded magnetic films should allow for a very significant tuning of the reorientation transition, because the actual depth-dependence of the magnetic state can be changed.

Moreover, the dynamic magnetic properties have still to be explored. In this regard, spin-wave (SW) is a topic of extensive research [159-161], which targets magnons to find alternatives for standard computing technology [162-164]. The SW band structure can be enriched with the artificial modulation of the magnetic media [165-169]. Recently, it has been

experimentally proven that SWs in FM thin films can exhibit a frequency non-reciprocity due to the interfacial Dzyaloshinskii–Moriya interaction (DMI) [170], opening new functionalities for magnon-based devices [171-173]. Such frequency non-reciprocity can be also induced by dipolar interaction, as for instance in FM films where the spatial symmetry is broken along the thickness [174,175], suggesting that non-reciprocity could be extended to FM layers exhibiting magnetic graduation along their thickness. Gallardo et al. [176] have recently made progress in this field, developing a theoretical approach to study and predict spin-wave dynamics of magnetization-graded ferromagnetic films. The proposed sample structure is depicted in Fig. 9(a), where the magnetization changes linearly along the film thickness as displayed in Fig. 9(b). It was interestingly found that the SW dispersion can be significantly modified, and that the degree of magnetization grading induces and controls the frequency non-reciprocity of two counter propagating spin waves. This is shown in the illustrative graph of Fig. 9(c), where two Damon–Eshbach (DE) modes, carrying the same *k*-vector, are found to precess at two different frequencies [176]. The findings of Ref. 176 opens therefore un unexplored design route for any technology, whose performances are impacted by such frequency difference $\Delta f = f(k) - f(-k)$, since Δf can now be accessed as a material tuning parameter by properly design the magnetization depth profile.

Future work in graded magnetic materials will also focus on thin film technology, which has been a core component of the information age. Although it has reached a high level of refinement, the hardware limitations imposed on HDD evolution have stimulated the development of other solutions for data storage such for instance strings of magnetic domains within nanowires [177], or the so-called Skyrmions, i.e., non collinear arrays of magnetic moments on the nanoscale [178]. At interfaces between magnetic layers and heavy metals [Fig. 10(a)] DMI can be strong enough to stabilize non-collinear spin textures or Skyrmions [179]. However, any real multilayer presents imperfections at each interface that can strongly affect the Skyrmion existence, characteristic, and reproducibility. Likewise, interfaces are the only portions that can be influenced in such multilayer structures, inherently limiting the total active contributions to a small fraction of the entire material. Thusly, it can be envisioned an innovative approach by means of graded magnetic metamaterials hosting pre-defined composition structures, mimicking the expansion of an interface hosting DMI into the entirety of the bulk of the film [Fig. 10(a)], and as such making a “pure” all-interface-metamaterial. Fig. 10(b) shows an exemplary ferromagnetic alloy layers with specific asymmetric and periodic compositional depth profiles, in which the spatial inversion symmetry is broken along the normal direction solely by the composition profile, which will give rise to designed

distribution of DMI. Such compositional profile could also be engineering in terms of its periodicity, amplitude, and shape. By doing so nanoscale design rules could be created to control the characteristic of non collinear spin textures, as depicted in the Fig. 10(c), in which the dimension of a Skyrmion is controlled by the compositional periodicity.

All in all, there is plenty of room to develop and exploit the intriguing properties of graded magnetic materials calling for intense interdisciplinary work, from modelling, magnonics, and surface science measurements to the chemical design of new suitable composition profiles.

Acknowledgments

L. F. acknowledge support from the Spanish Ministry of Science and Innovation under the Maria de Maeztu Units of Excellence Programme (Grant No. MDM-2016-0618) and Projects No. FIS2015-64519-R (MINECO/FEDER) and No. RTI2018-094881-B-100 (MCIU/Feder).

Figure captions

FIG. 1.(a) schematic showing the saturation magnetization M_S depth profile, while (b) displays the magnetic anisotropy K for an exemplary exchange spring structure. (c) Illustration of an exchange-spring state in a hard-magnetic/soft-magnetic bilayer at the blue dot in (d). (d) Exemplar magnetization reversal curve for a system exhibiting M_S and K profiles as in (a) and (b) where the irreversible part is highlighted in red.

FIG. 2. Schematics of the basic principle of graded anisotropy spring media, which show the possibility of keeping the same thermal stability (energy barrier) between two stable states while changing the required field to change the magnetization state [74].

FIG. 3.(a) Schematic of the depth-dependent exchange strength J normalized to its maximum for the (111) textured $Ni_{x(z)}Cu_{1-x(z)}$ thin alloy film devised in Ref. 97, whose layer stack is schematically shown as inset. (b), (c) Corresponding magnetization profiles at $T = 0.84 \cdot T_C$ and $T = 0.91 \cdot T_C$. Adapted from Ref. 97.

FIG. 4.(a) Schematic of the sample structure devised in Ref. 115 and relative magnetic moments above the critical temperature T_C of the central graded interlayer. The corresponding exchange strength J profile of the $Ni_{x(z)}Cu_{1-x(z)}$ interlayer is displayed directly into (a). (b) shows schematically the respective relative orientations of the magnetic moments throughout the entire stack for $T < T_C$ of the central $Ni_{x(z)}Cu_{1-x(z)}$ graded interlayer.

FIG. 5. (a) Schematic of the layer stack studied in Ref. 119, while (b) shows the Cr content depth profile of the CoCr graded magnetic layer. (c) – (i) shows data for the sample with Cr concentrations $x_c = 0.28$. (c) XRD θ-2θ scans normalized to the intensity of the Ag (220) peak. (d) Color-coded maps of the RT-IP angular dependence of the magnetization measured from saturation down to remanence [119]. (e) Corresponding least-squares fits of the data in (d) based upon the minimization of the total energy using a macrospin model [98]. (f) VSM-RT hysteresis loops (black dots) and MOKE measurements (red dashed lines) along the EA. The data are normalized according to Ref. 119. (g) Field- and temperature-dependence of the EA-magnetization for the hysteresis loop branches with decreasing field strengths: M/M_S equal to 1 represents positive magnetic saturation PP (yellow colour), −1 indicates negative saturation PN (blue colour), 0 corresponds to the antiparallel case AP (green colour). (h) and (i) field-dependent magnetic depth profile as determined from PNR data. Adapted from Ref. 119.

FIG. 6. (a) Schematic of the sample structure studied in Ref. 139. (b) displays the corresponding exchange strength J profile of the multilayer structure. (c) An illustration of the temperature dependence of the magnetization in two distinct alloy samples sharing the same material stoichiometry as in (a). (d) depicts schematically the magnetization depth profiles of the multilayers [139].

FIG. 7. (a) Schematic of the layer growth sequence for the samples studied in Ref. 144 . On the right the Ru modulations for the $\lambda = 10$ nm and $\lambda = 5$ nm cases. (b) normalized XRD θ–2θ scans to the intensity of the Ag (220) peaks. (c)-(d) angular dependence of the normalized magnetization as a function of the IP applied field angle and strength for $\lambda = 10$ nm (c), $\lambda = 20$ nm (d); (e)-(f) show the corresponding least-squares fits of the data using a macrospin model [98]. (g) Temperature-dependent magnetizations of the modulated and reference homogenous alloy samples, as measured by SQUID in $\mu_0 H = 5$ mT. Adapted from Ref. 144 and 150.

FIG. 8. PNR data, measured at T = 50 K in $\mu_0 H = 500$ mT along the EA, for $\lambda = 10$ nm (a), $\lambda = 5$ nm (c), which were fitted using the scattering length density (black straight lines) and magnetization depth profiles (red straight lines) of (b) and (d). (e) Schematic representing the unit cell used for the Mean Field (MF) model [144]. (f) Exchange strength J profile of the model unit cell. (g) Local Curie temperature modulation Δt_C as a function of exchange delocalization distance d_{dl}. Solid lines correspond to the MF model. Open symbols correspond to measured values from Ref. 144. Yellow shaded area indicates range of uncertainty in d_{dl} corresponding to two standard deviations. Adapted from Ref. 144 and 150.

FIG. 9. (a) Schematic view of SW excitation for a ferromagnetic film with a continuous variation of M along the thickness. The circular arrows indicate the magnetic field lines around the electric leads. (b) Schematic representation of the corresponding magnetization profile M(z). (c) Exemplar Damon–Eshbach (DE) SW dispersion [176] of a film exhibiting the magnetization profile in (b). The points refer to DE modes for the respective cases of a positive $+k$ (blue) and negative $-k$ (yellow).

FIG. 10. (a) the left shows a bilayer system in which the DMI vector **d** is at the Co/Pt interface. The right part shows a schematic of an "all-interface-bulk" metamaterial $FM_{1-x-y}A_xB_y$ (FM = ferromagnet and A ≠ B = heavy metals), with arrows mimicking the mesoscopic DMI $\mathbf{d}_n$ in the entire structure. (b) displays 3D-plot created from sets of (A at.%, B at.%, depth of $FM_{1-x-y}A_xB_y$) triples. (c) The upper part shows a cross sectional view of a skyrmion while the bottom displays three nanostripes hosting different skyrmion densities due to the different compositional profile within each stripe.

Figure 1

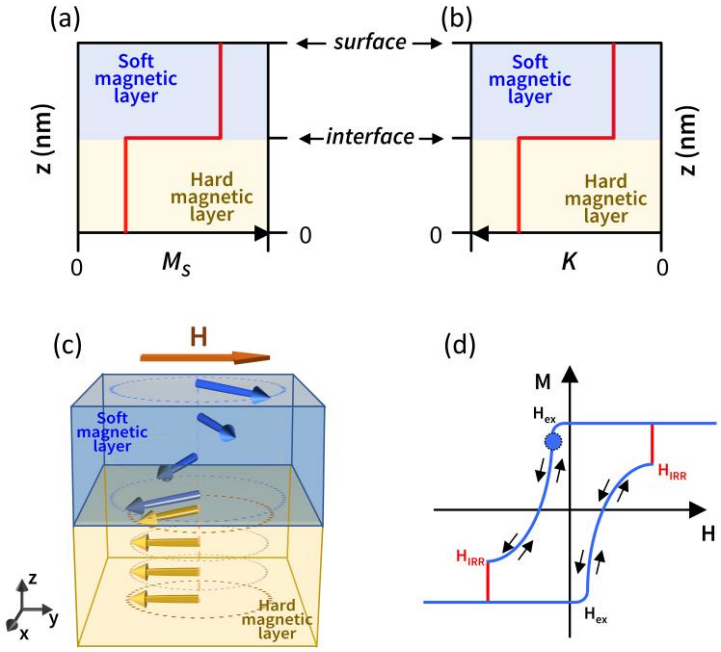
(a)
(b)
surface
interface
Soft magnetic layer
Hard magnetic layer
z (nm)
0
M_S
K
(c)
H
Soft magnetic layer
Hard magnetic layer
z
y
x
(d)
M
H_{ex}
H_{IRR}
H

Figure 2

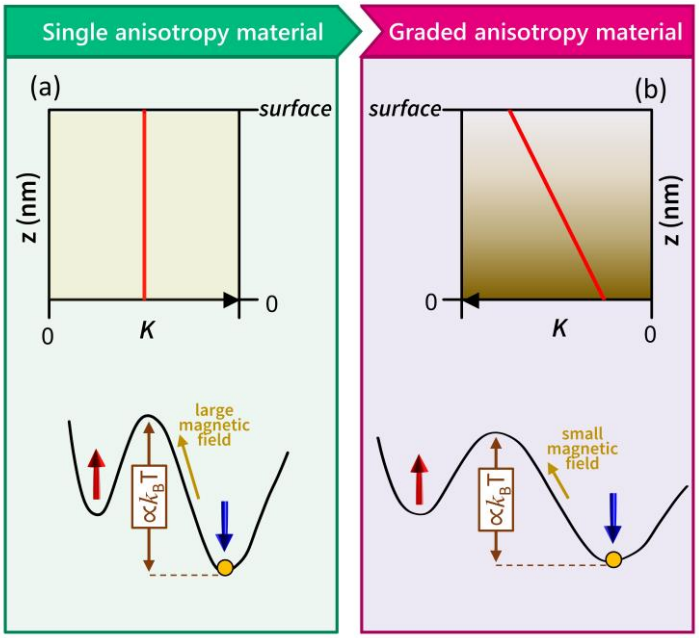
Single anisotropy material
Graded anisotropy material
(a)
surface
z (nm)
0
K
0
large magnetic field
$\propto k_B T$
(b)
surface
z (nm)
0
K
0
small magnetic field
$\propto k_B T$

Figure 3

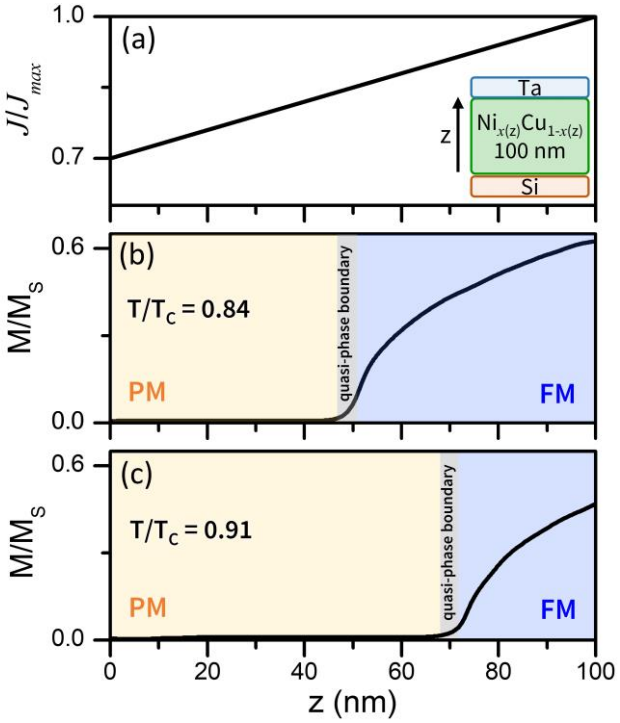
(a)
J/J_max
1.0
0.7
Ta
Ni_x(z)Cu_1-x(z)
100 nm
Si
z
(b)
M/M_S
0.6
0.0
T/T_C = 0.84
PM
FM
quasi-phase boundary
(c)
T/T_C = 0.91
0
20
40
60
80
100
z (nm)

Figure 4

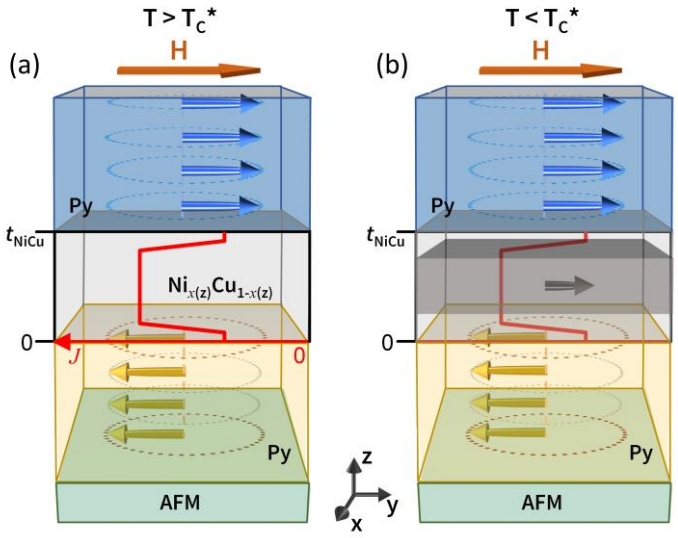
T > T$_C$*
H
(a)
Py
t_{NiCu}
$Ni_{x(z)}Cu_{1-x(z)}$
0
J
0
Py
AFM
T < T$_C$*
H
(b)
Py
t_{NiCu}
0
Py
AFM
z
y
x

Figure 5

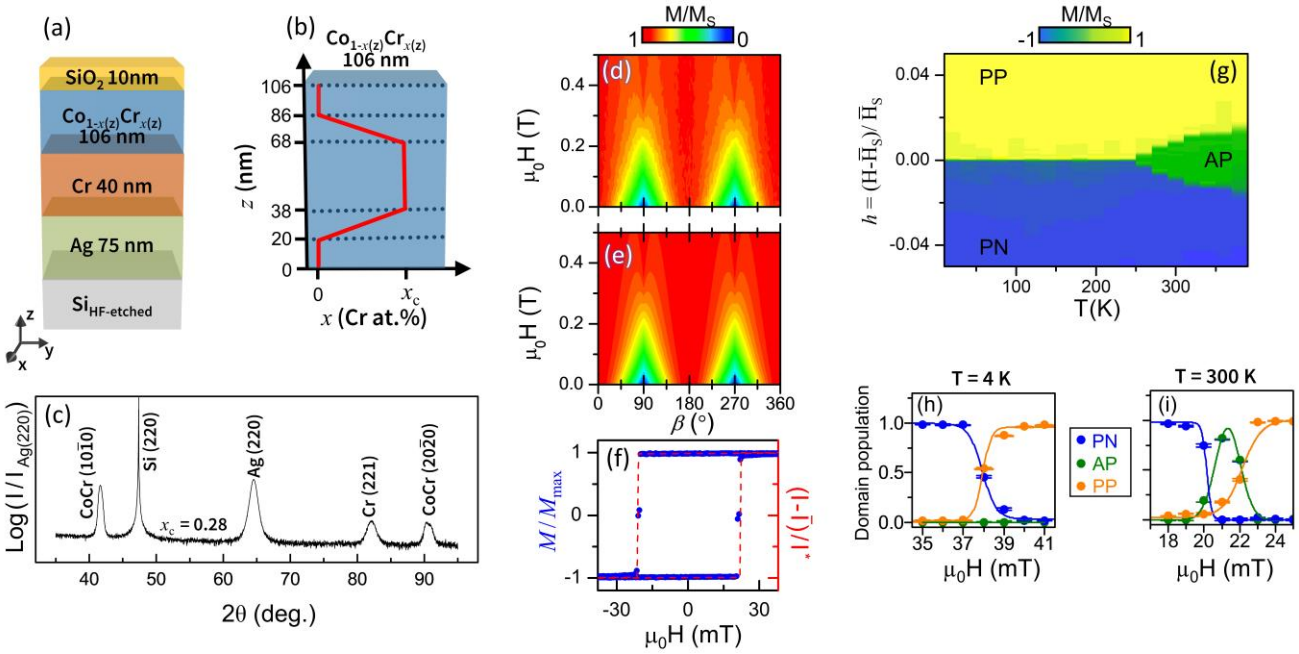
(a)
SiO2 10nm
Co1-x(z)Crx(z) 106 nm
Cr 40 nm
Ag 75 nm
SiHF-etched
z
x
y
(b)
Co1-x(z)Crx(z) 106 nm
106
86
68
38
20
0
z (nm)
0
xc
x (Cr at.%)
(c)
Log(I / IAg(220))
CoCr (10$\bar{1}$0)
Si (220)
Ag (220)
Cr (221)
CoCr (20$\bar{2}$0)
xc = 0.28
40
50
60
70
80
90
2θ (deg.)
M/MS
1
0
(d)
(e)
μ0H (T)
0.4
0.2
0.0
0
90
180
270
360
β (°)
(f)
M/Mmax
1
0
-1
-30
0
30
μ0H (mT)
I*/(I-1)
M/MS
-1
1
(g)
PP
AP
PN
0.04
0.00
-0.04
h = (H-H̄S)/ H̄S
100
200
300
T(K)
T = 4 K
(h)
Domain population
1.0
0.5
0.0
35
37
39
41
μ0H (mT)
PN
AP
PP
T = 300 K
(i)
18
20
22
24
μ0H (mT)

Figure 6

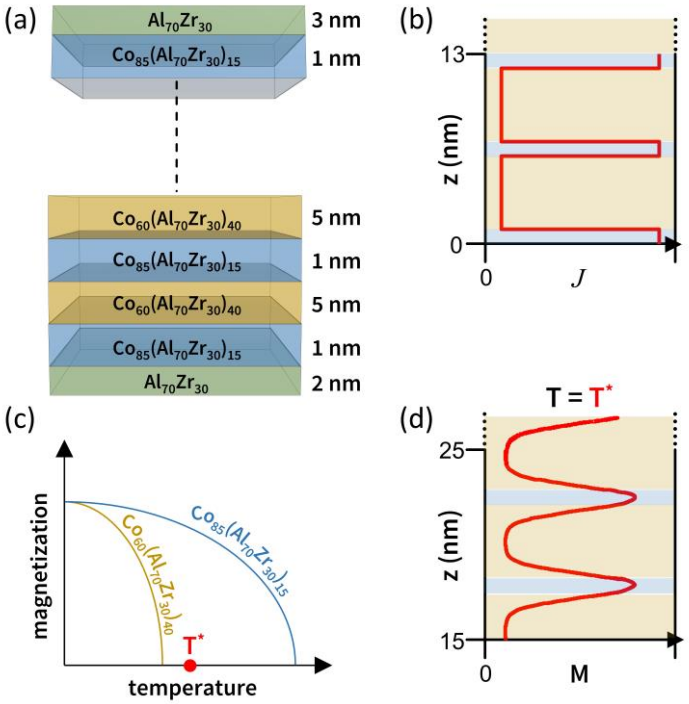
(a)
Al70Zr30
3 nm
Co85(Al70Zr30)15
1 nm
Co60(Al70Zr30)40
5 nm
Co85(Al70Zr30)15
1 nm
Co60(Al70Zr30)40
5 nm
Co85(Al70Zr30)15
1 nm
Al70Zr30
2 nm
(b)
13
z (nm)
0
0
J
(c)
magnetization
Co85(Al70Zr30)15
Co60(Al70Zr30)40
T*
temperature
(d)
T = T*
25
z (nm)
15
0
M

Figure 7

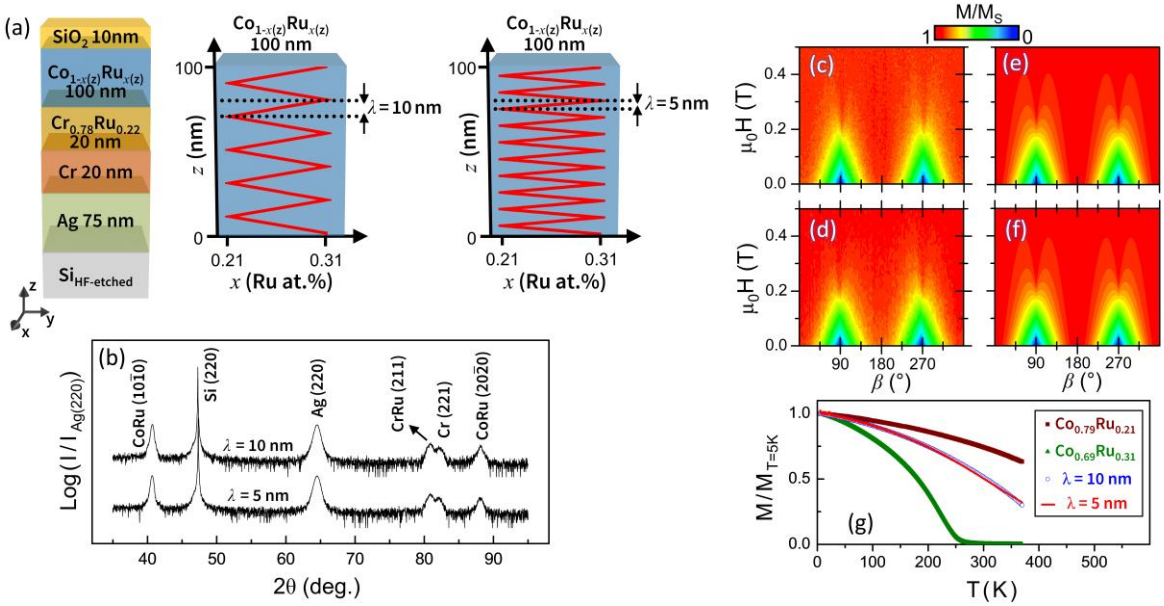
(a)
SiO2 10nm
Co1-x(z)Rux(z) 100 nm
Cr0.78Ru0.22 20 nm
Cr 20 nm
Ag 75 nm
SiHF-etched
z
y
x
Co1-x(z)Rux(z) 100 nm
100
z (nm)
0
0.21
0.31
x (Ru at.%)
λ = 10 nm
Co1-x(z)Rux(z) 100 nm
100
z (nm)
0
0.21
0.31
x (Ru at.%)
λ = 5 nm
(b)
Log (I / IAg(220))
CoRu (10$\bar{1}$0)
Si ($\bar{2}$20)
Ag (220)
CrRu (211)
Cr (221)
CoRu (20$\bar{2}$0)
λ = 10 nm
λ = 5 nm
40
50
60
70
80
90
2θ (deg.)
M/MS
1
0
(c)
(e)
(d)
(f)
μ0H (T)
0.4
0.2
0.0
90
180
270
β (°)
M/MT=5K
1.0
0.5
0.0
(g)
0
100
200
300
400
500
T (K)
Co0.79Ru0.21
Co0.69Ru0.31
λ = 10 nm
λ = 5 nm

Figure 8

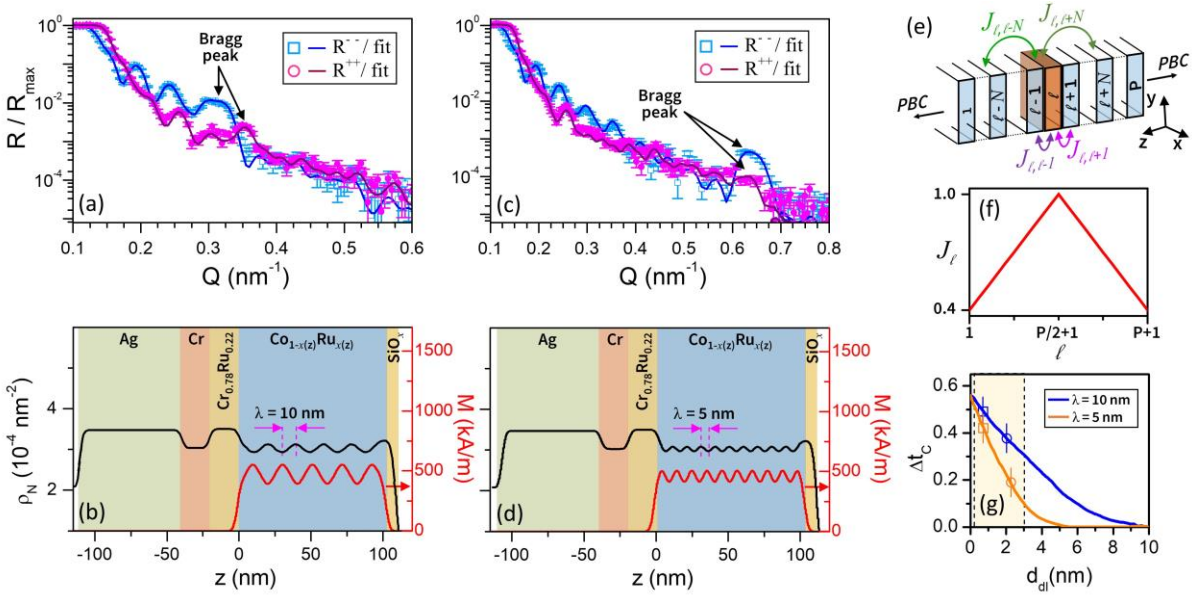
R / R_max
Bragg peak
R⁻⁻ / fit
R⁺⁺ / fit
(a)
(c)
Q (nm⁻¹)
(e)
PBC
(f)
J_ℓ
ℓ
(g)
Δt_C
d_dl(nm)
λ = 10 nm
λ = 5 nm
Ag
Cr
Cr0.78Ru0.22
Co1-x(z)Rux(z)
SiOx
ρN (10⁻⁴ nm⁻²)
M (kA/m)
(b)
(d)
z (nm)

Figure 9

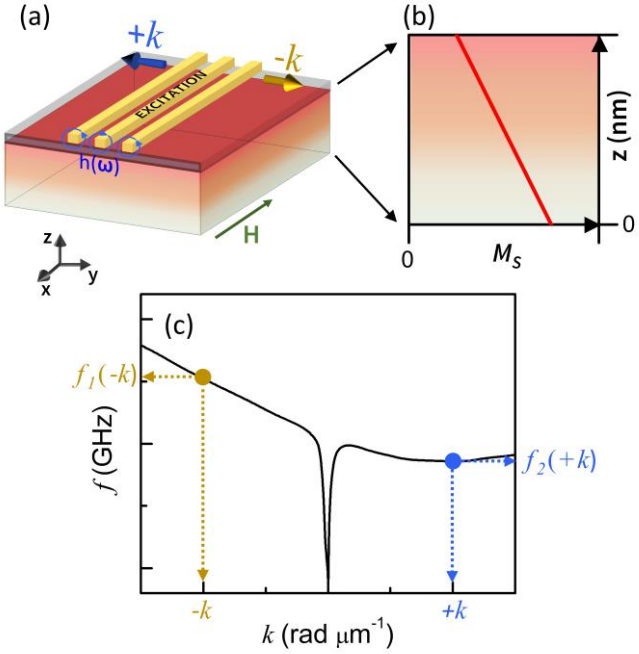

Figure 10

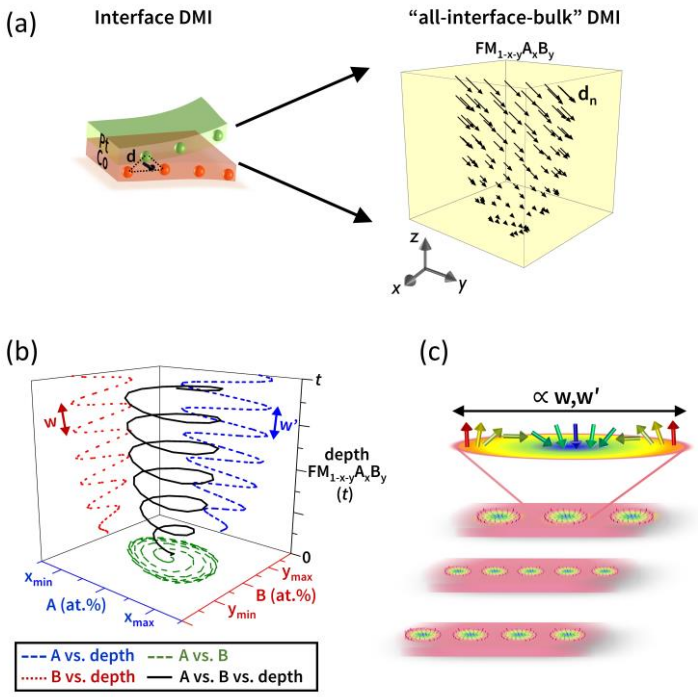
(a)
Interface DMI
"all-interface-bulk" DMI
Pt
Co
d
FM1-x-yAxBy
dn
z
x
y
(b)
t
w
w'
depth
FM1-x-yAxBy
(t)
0
xmin
A (at.%)
xmax
ymax
B (at.%)
ymin
A vs. depth
A vs. B
B vs. depth
A vs. B vs. depth
(c)
∝ w,w'

References

[1] J. P. Liu, E. Fullerton, O. Gutfleisch, and D. J. Sellmyer, "Nanoscale Magnetic Materials and Applications" (Springer, Dordrecht-Heidelberg-London-New York, 2009).

[2] O. Hellwig, A. Berger, J. B. Kortright, and E. E. Fullerton, "Domain structure and magnetization reversal of antiferromagnetically coupled perpendicular anisotropy films" *J. Magn. Magn. Mat.* **319**, 13-55 (2007).

[3] O. Hellwig, T. L. Kirk, J. B. Kortright, A. Berger, and E. E. Fullerton. "A new phase diagram for layered antiferromagnetic films" *Nat. Mat.* **2**, 112-116 (2003).

[4] B. Böhm, L. Fallarino, D. Pohl, B. Rellinghaus, K. Nielsch, N. S. Kiselev, and O. Hellwig, "Antiferromagnetic domain wall control via surface spin flop in fully tunable synthetic antiferromagnets with perpendicular magnetic anisotropy" *Phys. Rev. B* **100**, 140411 (2019).

[5] F. Kneller and R. Hawig, "The exchange-spring magnet: a new material principle for permanent magnets" *IEEE Trans. Magn.* **27**, 3588 (1991).

[6] R. Skomski and J. M. D. Coey, "Giant energy product in nanostructured two-phase magnets" *Phys. Rev. B* **48**, 15812 (1993).

[7] E. E. Fullerton, J. S. Jiang, S. D. Bader, "Hard/soft magnetic heterostructures: model exchange-spring magnets" *J. Magn. Magn. Mat.* **200**, 392-404 (1999).

[8] B. Saleh, J. Jiang, R. Fathi, T. Al-hababi, Q. Xu, L. Wang, D. Song, and A. Ma, "30 Years of functionally graded materials: An overview of manufacturing methods, Applications and Future Challenges" *Composites Part B* **201**, 108376 (2020).

[9] A. Sola, D. Bellucci, and V. Cannillo, "Functionally graded materials for orthopedic applications-an update on design and manufacturing" *Biotechnol. Adv.* **34**, 504–31 (2016).

[10] U. G. K. Wegst, H. Bai, E. Saiz, A. P. Tomsia, and R. O. Ritchie, "Bioinspired structural materials" *Nat. Mater.* **14**, 23 (2014).

[11] M. Eder, K. Jungnikl, and I. Burgert, "A close-up view of wood structure and properties across a growth ring of Norway spruce (Picea abies [L] Karst.) " *Trees* **23**, 79 (2009).

[12] M. K. Habibi, A. T. Samaei, B. Gheshlaghi, J. Lu, and Y. Lu, "Asymmetric flexural behavior from bamboo's functionally graded hierarchical structure: Underlying mechanisms" *Acta Biomater.* **16**, 178 (2015).

[13] J. Fidler, T. Schrefl, S. Hoefinger, M. Hajduga, "Recent developments in hard magnetic bulk materials" *J. Phys. Condens. Matter* **16**, S455 (2004).

[14] J. M. D. Coey, "Hard Magnetic Materials: A Perspective" *IEEE Trans. Magn.* **47**, 4671-4681 (2011).

[15] R. Wood, "The feasibility of magnetic recording at 1 terabit per square inch" *IEEE Trans. Magn.* **36**, 36–42 (2000).

[16] A. Berger, "Magnetization reversal in granular thin films" *Physica B* **407**, 1322–1329 (2012).

[17] T. J. Zhou, B. C. Lim, and B. Liu, "Anisotropy graded FePt-TiO_2 nanocomposite thin films with small grain size" *Appl. Phys. Lett.* **94**, 152505 (2009).

[18] M. Marcellini, M. Pärnaste, B. Hjörvarsson, M. Wolff, "Influence of the distribution of the inherent ordering temperature on the ordering in layered magnets" *Phys. Rev. B* **79**, 144426 (2009).

[19] J. S. Chen, L. S. Huang, J. F. Hu, G. Ju, and G. M. Chow, "FePt-C graded media for ultra-high density magnetic recording" *J. Phys. D Appl. Phys.* **43**, 185001 (2010).

[20] B. J. Kirby, J. E. Davies, K. Liu, S. M. Watson, G. T. Zimanyi, R. D. Shull, P. A. Kienzle, and J. A. Borchers, "Vertically graded anisotropy in Co/Pd multilayers" *Phys. Rev. B* **81**, 100405(R) (2010).

[21] A. Fert, "Nobel Lecture: Origin, development, and future od spintronics" *Rev. Mod. Phys.* **80**, 1517 (2008).

[22] P. A. Grünberg, "Nobel Lecture: From spin waves to giant magnetoresistance and beyond" *Rev. Mod. Phys.* **80**, 1531 (2008).

[23] E. Y. Tsymbal and D. G. Pettifor, "Perspectives of giant magnetoresistance" *Solid State Physics* **56**, 113–237 (2001).

[24] B. Dieny, "Giant magnetoresistance in spin-valve multilayers" *J. Magn. Magn. Mat.* **136**, 335-359 (1994).

[25] S. S. P. Parkin, C. Kaiser, A. Panchula, P. M. Rice, B. Hughes, M. Samant, and S.-H. Yang, "Giant tunnelling magnetoresistance at room temperature with MgO (100) tunnel barriers" *Nat. Mat.* **3**, 862–867 (2004).

[26] I. R. McFadyen, E. E. Fullerton, and M. J. Carey, "State-of-the-Art Magnetic Hard Disk Drives" *MRS Bulletin* **31**, 379–383 (2006).

[27] E. E. Fullerton and J. R Childress, "Spintronics, magnetoresistive heads, and the emergence of the digital world" Proc. IEEE **104**, 1787-1795 (2016).

[28] F. Hellman, A. Hoffman, G. S. D. Beach, E. E. Fullerton, C. Leighton, A. H. MacDonald, D. C. Ralph, D. A. Arena, H. A. Dürr, P. Fischer, J. Grollier, J. P. Heremans, T. Jungwirth, A. V. Kimel, B. Koopmans, I. N. Krivotorov, S. J. May, A. K. Petford-Long, J. M. Rondinelli, N. Samarth, I. K. Schuller, A. N. Slavin, M. D. Stiles, O. Tchemyshyov, A. Thiaville, and B. L. Zink, "Interface-induced phenomena in magnetism" *Rev. Mod. Phys.* **89**, 025006 (2017).

[29] A. Berger, S. Mangin, J. McCord, O. Hellwig, and E. E. Fullerton, "Cumulative minor loop growth in Co/Pt and Co/Pd multilayers" *Phys. Rev. B* **82**, 104423 (2010).

[30] L. Fallarino, A. Oelschlägel, J. A. Arregi, A. Bashkatov, F. Samad, B. Böhm, K. Chesnel, and O. Hellwig, "Control of domain structure and magnetization reversal in thick Co/Pt multilayers" *Phys. Rev. B* **99**, 024431 (2019).

[31] K. Chesnel, A. S. Westover, C. Richards, B. Newbold, M. Healey, L. Hindman, B. Dodson, K. Cardon, D. Montealegre, J. Metzner, T. Schneider, B. Böhm, F. Samad, L. Fallarino, and O. Hellwig, "Morphological stripe-bubble transition in remanent magnetic domain patterns of Co/Pt multilayer films and its dependence on Co thickness" Phys. Rev. B **98**, 224404 (2018).

[32] C. M. Günther, F. Radu, A. Menzel, S. Eisebitt, W. F. Schlotter, R. Rick, J. Lüning, and O. Hellwig, "Steplike versus continuous domain propagation in Co/Pd multilayer films" *Appl. Phys. Lett.* **93**, 072505 (2008).

[33] D. Weller, J. Stöhr, R. Nakajima, A. Carl, M. G. Samant, C. Chappert, R. Mégy, P. Beauvillain, P. Veillet, and G. A. Held, "Microscopic Origin of Magnetic Anisotropy in Au/Co/Au Probed with X-Ray Magnetic Circular Dichroism" *Phys. Rev. Lett.* **75**, 3752 (1995).

[34] L. Fallarino, S. Stienen, R. A. Gallardo, J. A. Arregi, V. Uhlíř, K. Lenz, R. Hübner, A. Oelschlägel, O. Hellwig, and J. Lindner, "Higher-order ferromagnetic resonances in out-of-plane saturated Co/Au magnetic multilayers" *Phys. Rev. B* **102**, 094434 (2020).

[35] J. U. Thiele, S. Maat, and E. E. Fullerton, "FeRh/FePt exchange spring films for thermally assisted magnetic recording media" *Appl. Phys. Lett.* **82**, 2859 (2003).

[36] J.-U. Thiele, S. Maat, J. L. Robertson, and E. E. Fullerton, "Magnetic and Structural Properties of FePt–FeRh Exchange Spring Films for Thermally Assisted Magnetic Recording Media", *IEEE Trans. Magn.* **40**, 2537 (2004).

[37] I. Suzuki, I. Suzuki, Y. Hamasaki, M. Itoh, and T. Taniyama, "Controllable exchange bias in Fe/metamagnetic FeRh bilayers", *Appl. Phys. Lett.* **105**, 172401 (2014).

[38] P. Dróżdż, M. Ślęzak, K. Matlak, B. Matlak, K. Freindl, D. Wilgocka-Ślęzak, N. Spiridis, J. Korecki, and T. Ślęzak, "Switching of Co Magnetization Driven by Antiferromagnetic-Ferromagnetic Phase Transition of FeRh Alloy in Co/FeRh Bilayers", *Phys. Rev. Appl.* **9**, 034030 (2018).

[39] Y. Xie, Q. Zhan, Y. Hu, X. Hu, X. Chi, C. Zhang, H. Yang, W. Xie, X. Zhu, J. Gao, W. Cheng, D. Jiang, and R.-W. Li, "Magnetocrystalline anisotropy imprinting of an antiferromagnet on an amorphous ferromagnet in FeRh/CoFeB heterostructures" *NPG Asia Mater*. **12**, 67 (2020).

[40] S. Yamada, K. Tanikawa, J. Hirayama, T. Kanashima, T. Taniyama, and K. Hamaya, "Exchange coupling in metallic multilayers with a topFeRh layer" AIP Advances **6**, 056115 (2016).

[41] G. Ju, Y. Peng, E. K. C. Chang, Y. Ding, A. Q. Wu, X. Zhu, Y. Kubota, T. J. Klemmer, H. Amini, L. Gao, Z. Fan, T. Rausch, P. Subedi, M. Ma, S. Kalarickal, C. J Rea, D. V. Dimitrov, P.-W. Huang, K. Wang, X. Chen, C. Peng, J. W. Dykes, M. A. Seigler, E. C. Gage, R. Chantrell, and J.-U. Thiele, "High Density Heat Assisted Magnetic Recording Media and Advanced Characterization-Progress and Challenges" *IEEE Trans. Magn.* **51**, 3201709 (2015).

[42] D. Weller, G. Parker, O. Mosendz, E. Champion, B. Stipe, X. Wang, T. Klemmer, G. Ju, and A. Ajan, "A HAMR Media Technology Roadmap to an Areal Density of 4 Tb/in" *IEEE Trans. Magn.* **50**, 1-8 (2014).

[43] X. He, Y. Wang, N. Wu, A. N. Caruso, E. Vescovo, K. D. Belashchenko, P. A. Dowben, and C. Binek, "Robust isothermal electric control of exchange bias at room temperature" *Nat. Mat.* **9**, 579–585 (2010).

[44] M. Street, W. Echtenkamp, Takashi Komesu, Shi Cao, P. A. Dowben, and Ch. Binek "Increasing the Néel temperature of magnetoelectric chromia for voltage-controlled spintronics" *Appl. Phys. Lett.* **104**, 222402 (2014).

[45] L. Fallarino, A. Berger, C. Binek, "Giant temperature dependence of the spin reversal field in magnetoelectric chromia" *Appl. Phys. Lett.* **104**, 022403 (2014).

[46] L. Fallarino, C. Binek, A. Berger, "Boundary magnetization properties of epitaxial $Cr_{2-x}Al_xO_3$ thin films" *Phys. Rev. B* **91**, 214403 (2015).

[47] A. Aharoni, "Reduction in coercive force caused by a certain type of imperfection" *Phys. Rev.* **119**, 127 (1960); C. Abraham and A. Aharoni, "Linear decrease in the magnetocrystalline anisotropy" *ibid.* 120, 1576 (1960).

[48] E. Goto, N. Hayashi, T. Miyashita, and K. Nakagawa "Magnetization and Switching Characteristics of Composite Thin Magnetic Films" *J. Appl. Phys.* **36**, 2951–2958 (1965).

[49] K. Mibu, T. Nagahama, and T. Shinjo, "Reversible magnetization process and magnetoresistance of soft-magnetic (NiFe) / hard-magnetic (CoSm) bilayers," *J. Magn. Magn. Mater.* **163**, 75 (1996).

[50] "Ultra-High-Density Magnetic Recording: Storage Materials and Media Designs" edited by G. Varvaro and F. Casoli (Pan Stanford, 2016).

[51] F. Herbst, "R2Fe14B materials: Intrinsic properties and technological aspects" *Rev. Mod. Phys.* **63**, 819 (1991).

[52] M. D. Coey and R. Skomski, "New magnets from interstitial intermetallics" *Phys. Scripta* **T49**, 315 (1993).

[53] A. Y. Dobin and H. J. Richter, "Domain wall assisted magnetic recording" *J. Appl. Phys.* **101**, 09K108 (2007).

[54] D. Goll and S. Macke, "Thermal stability of ledge-type $L1_0$-FePt/Fe exchange-spring nanocomposites for ultrahigh recording densities" Appl. Phys. Lett. **93**, 152512 (2008).

[55] D. Goll and H. Kronmüller, "Critical fields of an exchange coupled two-layer composite particle" Physica B: Condens. Matter. **403**, 1854–1859 (2008).

[56] D. Goll, S. Macke, and H. Kronmueller, "Exchange coupled composite layers for magnetic recording" Physica B: Condens. Matter. **403**, 338–341 (2008).

[57] F. Casoli, F. Albertini, L. Nasi, S. Fabbrici, R. Cabassi, F. Bolzoni, and C. Bocchi, "Strong coercivity reduction in perpendicular FePt/Fe bilayers due to hard/soft coupling" *Appl. Phys. Lett.* **92**, 142506 (2008).

[58] J.-L. Tsai, H.-T. Tzeng, and G.-B. Lin, "Magnetization reversal process in Fe/FePt films" Appl. Phys. Lett. **96**, 032505 (2010).

[59] D. Makarov, J. Lee, C. Brombacher, C. Schubert, M. Fuger, D. Suess, J. Fidler, and M. Albrecht, "Perpendicular FePt-based exchange-coupled composite media" Appl. Phys. Lett. **96**, 062501 (2010).

[60] J. S. Jiang, J. E. Pearson, Z. Y. Liu, B. Kabius, S. Trasobares, D. J. Miller, S. D. Bader, D. R. Lee, D. Haskel, G. Srajer, and J. P. Liu, "A new approach for improving exchange-spring magnets" *J. Appl. Phys.* **97**, 10K311s (2005).

[61] J. S. Jiang, S. D. Bader, H. Kaper, G. K. Leaf, R. D. Shull, A. J. Shapiro, V. S. Gornakov, V. I. Nikitenko, C. L. Platt, A. E. Berkowitz, S. David and E. E. Fullerton, "Rotational hysteresis of exchange-spring magnets" *J. Phys. D: Appl. Phys.* **35**, 2339–2343 (2002).

[62] V. E. Kuncser, M. Doi, W. Keune, M. Askin, H. Spies, J. S. Jiang, A. Inomata, and S. D. Bader, "Observation of the Fe spin spiral structure in Fe/Sm-Co exchange-spring bilayers by Mössbauer spectroscopy" *Phys. Rev. B* **68**, 064416 (2003).

[63] M. Moskalenko, P. F. Bessarab, V. M. Uzdin, and H. Jónsson, "Qualitative insight and quantitative analysis of the effect of temperature on the coercivity of a magnetic system" *AIP Advances* **6**, 025213 (2016).

[64] E. E. Fullerton, J. S. Jiang, and S. D. Bader, "Hard/soft magnetic heterostructures: model exchange-spring magnets" *J. Magn. Magn. Mat.* **200**, 392-404 (1999).

[65] E. E. Fullerton, J. S. Jiang, M. Grimsditch, C. H. Sowers, and S. D. Bader, "Exchange-spring behaviour in epitaxial hard/soft magnetic bilayers" *Phys. Rev. B* **58**, 12193 (1998).

[66] R. H. Victora and X. Shen, "Exchange coupled composite media for perpendicular magnetic recording" *IEEE Trans. Magn.* 41, 2828-2833 (2005).

[67] E. E. Fullerton, D. T. Margulies, N. Supper, H. Do, M. Schabes, A. Berger, and A. Moser, "Antiferromagnetically coupled magnetic recording media" *IEEE Trans. Magn.* **39**, 639 (2003).

[68] A. Berger, N. Supper, Y. Ikeda, B. Lengsfield, A. Moser, and E. E. Fullerton, "Improved media performance in optimally coupled exchange spring layer media" *Appl. Phys. Lett.* **93**, 122502 (2008).

[69] S. M. Mohseni, R. K. Dumas, Y. Fang, J. W. Lau, S. R. Sani, J. Persson, and J. Akerman, "Temperature-dependent interlayer coupling in Ni/Co perpendicular pseudo-spin-valve structures" *Phys. Rev. B* **84**, 174432 (2011).

[70] R. K. Dumas, Y. Fang, B. J. Kirby, C. Zha, V. Bonanni, J. Nogués, and J. Åkerman, "Probing vertically graded anisotropy in FePtCu films" *Phys. Rev. B* **84**, 054434 (2011).

[71] J. Zhang, Z. Sun, J. Sun, S. Kang, S. Yu, G. Han, S. Yan, L. Mei, and D. Li, "Structural and magnetic properties of patterned perpendicular media with linearly graded anisotropy" *Appl. Phys. Lett.* **102**, 152407 (2013).

[72] C. L. Zha, R. K. Dumas, Y. Y. Fang, V. Bonanni, and J. Nogúes, "Continuously graded anisotropy in single $(Fe53Pt47)_{100-x}Cu_x$ Films" *Appl. Phys. Lett.* **97**, 182504 (2010).

[73] D. Suess, “Multilayer exchange spring media for magnetic recording” *Appl. Phys. Lett.* **89**, 113105 (2006).

[74] D. Suess, J. Lee, J. Fidler, and T. Schrefl, “Exchange-coupled perpendicular media” *J. Magn. Magn. Mat.* **321**, 545–554 (2009).

[75] G. T. Zimanyi, “Graded media: Optimization and energy barriers” *J. Appl. Phys.* **103**, 07F543 (2008).

[76] D. Goll, A. Breitling, L. Gu, P. A. Van Aken, and W. Sigle, “Experimental realization of graded L10-FePt/Fe composite media with perpendicular magnetization” *J. Appl. Phys.* **104**, 083903 (2008).

[77] T. A. George, Y. Yu, L. Yue, R. Skomski, and D. J. Sellmyer, “Control of coercivity in exchange-coupled graded (001) FePt : SiO2 nanocomposite films” *IEEE Trans. Magn.* **46**, 2435–2437 (2010).

[78] V. Alexandrakis, T. Speliotis, E. Manios, D. Niarchos, J. Fidler, J. Lee, and G. Varvaro, “Hard/graded exchange spring composite media based on FePt” *J. Appl. Phys.* **109**, 07B729 (2011).

[79] C. J. Jiang, J. S. Chen, J. F. Hu, and G. M. Chow, “FePt-TiO2 exchange coupled composite media with well-isolated columnar microstructure for high density magnetic recording” *J. Appl. Phys.* **107**, 123915 (2010).

[80] V. Alexandrakis, D. Niarchos, K. Mergia, J. Lee, J. Fidler, and I. Panagiotopoulos, “Magnetic properties of graded A1/L10 films obtained by heat treatment of FePt/CoPt multilayers” *J. Appl. Phy.* **107**, 013903 (2010).

[81] T. A. George, Y. Yu, L. Yue, R. Skomski, D. J. Sellmyer, “Control of Coercivity in Exchange-Coupled Graded (001) FePt:SiO_2 Nanocomposite Films” IEEE Trans. Magn. **46**, 2435-2437 (2010).

[82] J. L. Tsai, H. T. Tzeng, and B. F. Liu, “Magnetic properties and microstructure of graded Fe/FePt films” *J. Appl. Phys.* **107**, 113923 (2010).

[83] F. Wang, X. -H. Xu, Y. Liang, J. Zhang, and J. Zhang, “Perpendicular L10-FePt/Fe and L10-FePt/Ru/Fe graded media obtained by post-annealing” *J. Mater. Chem. Phys.* **126**, 843 (2011).

[84] B. J. Kirby, S. M. Watson, J. E. Davies, G. T. Zimanyi, Kai Liu, R. D. Shull, and J. A. Borchers, “Direct observation of magnetic gradient in Co/Pd pressure graded media” *J. Appl. Phys* **105**, 07C929 (2009).

[85] C. L. Zha, R. K. Dumas, Y. Y. Fang, V. Bonanni, J. Nogues, and J. Åkerman, "Continuously graded anisotropy in single $(Fe_{53}Pt_{47})_{100-x}Cu_x$ films" *Appl. Phys. Lett.* **97**, 182504 (2010).

[86] V. Bonanni, Y. Fang, R. K. Dumas, C. Zha, S. Bonetti, J. Nogues, and J. Åkerman "First-order reversal curve analysis of graded anisotropy FePtCu films" *Appl. Phys. Lett.* **97**,202501 (2010).

[87] R. K. Dumas, C. Zha, Y. Fang, V. Bonanni, J. W. Lau, J. Nogues, and J. Åkerman "Graded anisotropy FePtCu films" *IEEE Trans. Magn.* **47**, 1580 (2011).

[88] Y.-H. Lin, J.-H. Hsu, F.-T. Yuan, P. C. Kuo, and J. K. Mei, "Microstructure and magnetic performance of perpendicularly magnetic anisotropic Fe3Pt/Fe2Pt/L10-FePt(001)/MgO(002) graded films" *IEEE Trans. Magn.* **49**, 3679–3682 (2013).

[89] F. Wang, J. Zhang, J. Zhang, C. Wang, Z. Wang, H. Zeng, M. Zhang, and X. Xu, "Graded/soft/graded exchange-coupled thin films fabricated by [FePt/C]5/Fe/[C/FePt]5 multilayer deposition and post-annealing" *Appl. Surf. Sci.* **271**, 390–393 (2013).

[90] A. di Bona, P. Luches, F. Albertini, F. Casoli, P. Lupo, L. Nasi, S. D'Addato, G. C. Gazzadi, and S.Valeri "Anisotropy-graded magnetic media obtained by ion irradiation of $L1_0$ FePt" *Acta Mater.* **61**, 4840–4847 (2013).

[91] J. Fassbender, J. Grenzer, O. Roshchupkina, Y. Choi, J. S. Jiang, S. D. Bader, "The effect of ion irradiation and annealing on exchange spring magnets" *J. Appl. Phys.* **105**, 023902 (2009).

[92] N. Gaur, K. K. M. Pandey, S. L. Maurer, S. N. Piramanayagam, R. W. Nunes, H. Yang, and C. S. Bhatia, "Magnetic and structural properties of CoCrPt–SiO2-based graded media prepared by ion implantation" *J. Appl. Phys.* **110**, 083917 (2011).

[93] C. Le Graët, T. R. Charlton, M. McLaren, M. Loving, S. A. Morley, C. J. Kinane, R. M. D. Brydson, L. H. Lewis, S. Langridge, and C. H. Marrows, "Temperature controlled motion of an antiferromagnet-ferromagnet interface within a dopant-graded FeRh epilayer" *APL Mater.* **3**, 041802 (2015).

[94] S. Y. Shiryaev, F. Jensen, and J. W. Petersen, "On the nature of cross-hatch patterns on compositionally graded $Si_{1-x}Ge_x$ alloy layers" *Appl. Phys. Lett.* **64**, 3305 (1994).

[95] F. K. LeGoues, B. S. Meyerson, J. F. Morar, and P. D. Kirchner, "Mechanism and conditions for anomalous strain relaxation in graded thin films and superlattices" *J. Appl. Phys.* **71**, 4230 (1992).

[96] E. A. Fitzgerald, Y.-H. Xie, D. Monroe, P. J. Silverman, J. M. Kuo, A. R. Kortan, F. A. Thiel, and B. E. Weir, "Relaxed Ge_xSi_{1-x} structures for III–V integration with Si and high mobility two-dimensional electron gases in Si" *J. Vat. Sci. Technol. B* **10**, 1807 (1992).

[97] B. J. Kirby, H. F. Belliveau, D. D. Belyea, P. A. Kienzle, A. J. Grutter, P. Riego, A. Berger, and Casey W. Miller "Spatial Evolution of the Ferromagnetic Phase Transition in an Exchange Graded Film" *Phys. Rev. Lett.* **116**, 047203 (2016).

[98] O. Idigoras, U. Palomares, A. K. Suszka, L. Fallarino, and A. Berger, "Magnetic properties of room temperature grown epitaxial $Co_{1-x}Ru_x$ alloy films" *Appl. Phys. Lett*. **103**, 102410 (2013).

[99] N. Inaba, Y. Uesaka, and M. Futamoto, "Compositional and temperature dependence of basic properties of CoCr-alloy thin films" *IEEE Trans. Magn.* **36**, 54–60 (2000).

[100] R. W. Wang and D. L. Mills, "Onset of long-range order in superlattices: mean-field theory" *Phys. Rev. B* 46,11681(1992).

[101] R. Skomski and D. J. Sellmyer, "Curie temperature of multiphase nanostructures" *J. Appl. Phys.* **87**, 4756 (2000).

[102] S. S. P. Parkin, "Systematic variation of the strength and oscillation period of indirect magnetic exchange coupling through the 3d, 4d, and 5d transition metals" *Phys. Rev. Lett.* **67**, 3598 (1991).

[103] A. Fert, P. Grünberg, A. Barthélémy, F. Petroff, and W. Zinn, "Layered magnetic structures: interlayer exchange coupling and giant magnetoresistance" *J. Magn. Magn. Mater.* **1**, 140–144 (1995).

[104] G. W. Fernando, "Metallic Multilayers and their Applications: Theory, Experiments, and Applications Related to Thin Metallic Multilayers, edited by G. W. Fernando, Handbook of Metal Physics Vol. 4 (Elsevier, Amsterdam, 2008).

[105] J. M. Daughton, "GMR applications" *J. Magn. Magn. Mater.* **192**, 334 (1999).

[106] J. C. Slonczewski, "Current-driven excitation of magnetic multilayers" *J. Magn. Magn. Mater*.**159**, L1-L7 (1996).

[107] E. B. Myers, D. C. Ralph, J. A. Katine, R. N. Louie, and R. A. Buhrman, "Current-Induced Switching of Domains in Magnetic Multilayer Devices" *Science* 285, 867-870 (1999).

[108] A. Brataas, A. D. Kent, and H. Ohno, Nat. Mater.11, 372 (2012).

[109] P. Grünberg, R. Schreiber, Y. Pang, M. B. Brodsky, and H. Sowers, "Layered magnetic structures: Evidence for antiferromagnetic coupling of Fe layers across Cr interlayers" *Phys. Rev. Lett.* 57, 2442 (1986).

[110] G. Binasch, P. Grünberg, F. Saurenbach, and W. Zinn, "Enhanced magnetoresistance in layered magnetic structures with antiferromagnetic interlayer exchange" *Phys. Rev. B* **39**, 4828 (1989).

[111] M. N. Baibich, J. M. Broto, A. Fert, F. Nguyen Van Dau, F. Petroff, P. Etienne, G. Creuzet, A. Friederich, and J. Chazelas, "Giant Magnetoresistance of (001)Fe/(001)Cr Magnetic Superlattices" *Phys. Rev. Lett.* **61**, 2472 (1988).

[112] L. Fallarino, V. Sluka, B. Kardasz, M. Pinarbasi, A. Berger, and A. D. Kent, "Interlayer exchange coupling between layers with perpendicular and easy-plane magnetic anisotropies" *Appl. Phys. Lett.* **109**, 082401 (2016).

[113] S. Andersson and V. Korenivski, "Thermoelectrically Controlled Spin-Switch" *IEEE Trans. Magn.* **46**, 2140 (2010).

[114] S. Andersson and V. Korenivski, "Exchange coupling and magnetoresistance in CoFe/NiCu/CoFe spin valves near the Curie point of the spacer" *J. Appl. Phys.* **107**, 09D711 (2010).

[115] A. F. Kravets, A. N. Timoshevskii, B. Z. Yanchitsky, M. A. Bergmann, J. Buhler, S. Andersson, and V. Korenivski, "Temperature-controlled interlayer exchange coupling in strong/weak ferromagnetic multilayers: A thermomagnetic Curie switch" *Phys. Rev. B* **86**, 214413 (2012).

[116] A. F. Kravets, Yu. I. Dzhezherya, A. I. Tovstolytkin, I. M. Kozak, A. Gryshchuk, Yu. O. Savina, V. A. Pashchenko, S. L. Gnatchenko, B. Koop, and V. Korenivski, "Synthetic ferrimagnets with thermomagnetic switching" *Phys. Rev. B* **90**, 104427 (2014).

[117] I. L. Prejbeanu, M. Kerekes, R. C. Sousa, H. Sibuet, O. Redon, B. Dieny, and J. P. Nozières, "Thermally assisted MRAM" *J. Phys.: Condens. Matter* **19**, 165218 (2007).

[118] C. Binek, "Training of the exchange-bias effect: A simple analytic approach" *Phys. Rev. B* **70**, 014421 (2004).

[119] L. Fallarino, B. J. Kirby, M, Pancaldi, P. Riego, A. L. Balk, C. W. Miller, P. Vavassori, and A. Berger, "Magnetic properties of epitaxial CoCr films with depth-dependent exchange-coupling profiles" *Phys. Rev. B* **95**, 134445 (2017).

[120] S. Honda, K. Takahashi, and T. Kusuda, “Wall energy and exchange stiffness in CoCr films sputtered on low temperature substrates” *Jap. J. Appl. Phys.* **26**, L593 (1987).

[121] N. Inaba, Y. Uesaka, and M. Futamoto, “Compositional and temperature dependence of basic magnetic properties of CoCr-alloy thin films” *IEEE Trans. Magn*. **36**, 54 (2000).

[122] S. Yuasa, T. Nagahama, A. Fukushima, Y. Suzuki, and K. Ando, “Giant room-temperature magnetoresistance in single-crystal Fe/MgO/Fe magnetic tunnel junctions” *Nat. Mater.* **3**, 868–871 (2004).

[123] N. Inaba, M. Futamoto, and A. Nakamura, “Temperature dependence of magnetocrystalline anisotropy energy determined using Co-Cr-Ta single crystal thin films” *IEEE Trans. Magn.* **34**, 1558–1560 (1998).

[124] I. Žutić, A. Matos-Abiague, B. Scharf, H. Dery, and K. Belashchenko, “Proximitized materials” *Mater. Today* **22**, 85–107 (2019).

[125] R. M. White and D. J. Friedman, “Theory of the magnetic proximity effect” *J. Magn. Magn. Mater.* **49**, 117 (1985).

[126] M. J. Zuckermann, “The proximity effect for weak itinerant ferromagnets” *Solid State Commun.* **12**, 745 (1973).

[127] P. K. Manna and S. M. Yusuf, “Two interface effects: Exchange bias and magnetic proximity” *Phys. Rep.* **535**, 61 (2014).

[128] U. Bovensiepen, F. Wilhelm, P. Srivastava, P. Poulopoulos, M. Farle, A. Ney, and K. Baberschke, “Two Susceptibility Maxima and Element Specific Magnetizations in Indirectly Coupled Ferromagnetic Layers” *Phys. Rev. Lett.* **81**, 2368 (1998).

[129] F. Magnus, M. E. Brooks-Bartlett, R. Moubah, R. A. Procter, G. Andersson, T. P. A. Hase, S. T. Banks, and B. Hjörvarsson, “Long-range magnetic interactions and proximity effects in an amorphous exchange-spring magnet” *Nat. Commun.* **7**, 11931 (2016).

[130] R. W. Wang and D. L. Mills, “Onset of long-range order in superlattices: Mean-field theory” *Phys. Rev. B* **46**, 11681 (1992).

[131] N. J. Gökemeijer, T. Ambrose, and C. L. Chien, “Long-Range Exchange Bias Across a Spacer Layer” *Phys. Rev. Lett.* **79**, 4270 (1997).

[132] M. A. Tomaz, W. J. Antel Jr, W. L. O’Brien, and G. R. Harp, “Induced V moments in Fe/V(100), (211), and (110) superlattices studied using x-ray magnetic circular dichroism” *J. Phys.: Condens. Matter* **9**, L179 (1997).

[133] H. Palonen, F. Magnus, and B. Hjörvarsson, “Double magnetic proximity in Fe0.32V0.68 superlattices” *Phys. Rev. B* **98**, 144419 (2018).

[134] L. Cheng, Z. Altounian, D. H. Ryan, J. O. Ström-Olsen, M. Sutton, and Z. Tun, “Pd polarization and interfacial moments in Pd-Fe multilayers” *Phys. Rev. B* **69**, 144403 (2004).

[135] W. L. Lim, N. Ebrahim-Zadeh, J. C. Owens, H. G. E. Hentschel, and S. Urazhdin, “Temperature-dependent proximity magnetism in Pt” *Appl. Phys. Lett.* **102**, 162404 (2013).

[136] O. Rader, E. Vescovo, J. Redinger, S. Blügel, C. Carbone, W. Eberhardt, and W. Gudat, “Fe-Induced Magnetization of Pd: The Role of Modified Pd Surface States” *Phys. Rev. Lett.* **72**, 2247 (1994).

[137] P. Sharma, H. Kimura, and A. Inoue, “Magnetic behavior of cosputtered Fe-Zr amorphous thin films exhibiting perpendicular magnetic anisotropy” *Phys. Rev. B* **78**, 134414 (2008).

[138] R. A. Procter, F. Magnus, G. Andersson, C. Sánchez-Hanke, B. Hjörvarsson, and T. Hase, “Magnetic leverage effects in amorphous SmCo/CoAlZr heterostructures” *Appl. Phys. Lett.* **107**, 062403 (2015).

[139] K. A. Thórarinsdóttir, H. Palonen, G. K. Palsson, B. Hjörvarsson, and F. Magnus, “Giant magnetic proximity effect in amorphous layered magnets” *Phys. Rev. Mat.* **3**, 054409 (2019).

[140] F. Magnus, R. Moubah, A. H. Roos, A. Kruk, V. Kapaklis, T. Hase, B. Hjörvarsson, and G. Andersson, “Tunable giant magnetic anisotropy in amorphous SmCo thin films” *Appl. Phys. Lett.* **102**, 162402 (2013).

[141] H. Raanaei, H. Nguyen, G. Andersson, H. Lidbaum, P. Korelis, K. Leifer, and B. Hjörvarsson, “Imprinting layer specific magnetic anisotropies in amorphous multilayers”, *J. Appl. Phys.* **106**, 023918 (2009).

[142] A. J. Qviller, C. Frommen, B. C. Hauback, F. Magnus, B. J. Kirby, and B. Hjörvarsson, “Direct observation of magnetic proximity effects in amorphous exchange-spring magnets by neutron reflectometry” *Phys. Rev. Materials* **4**, 104404 (2020).

[143] R. Gemma, M. to Baben, A. Pundt, V. Kapaklis, and B. Hjörvarsson, “The impact of nanoscale compositional variation on the properties of amorphous alloys” *Sci. Rep.* **10**, 11410 (2020).

[144] B. J. Kirby, L. Fallarino, P. Riego, B. B. Maranville, Casey W. Miller, and A. Berger, “Nanoscale magnetic localization in exchange strength modulated ferromagnets” *Phys. Rev. B* **98**, 064404 (2018).

[145] A.-C. Sun, J. -H. Hsu, C. H. Sheng, P. C. Kuo, H. L. Huang, "Grain size reduction by doping Cr underlayer with Ru for longitudinal magnetic recording media" *IEEE Trans. Magn.* **43**, 882–884 (2007).

[146] V. Pierron-Bohnes, N. Ringelstein, A. Michel, S. Boukari, L. Bouzidi, N. Persat, E. Beaurepaire, M. Hehn, D. Muller, and M. C. Cadeville, "Observation of an ordered new compound $Co_{1-x}Ru_x$ prepared by MBE on a Ru buffer layer" *J. Magn. Magn. Mat.* **165**, 176 (1997).

[147] H. Hashizume, K. Ishiji, J. C. Lang, D. Haskel, G. Srajer, J. Minár, and H. Ebert, "Observation of x-ray magnetic circular dichroism at the Ru *K* edge in Co-Ru alloys" *Phys. Rev. B* **73**, 224416 (2006).

[148] S. B. Qadri, T. M. Keller, M. Laskoski, C. A. Little, M. S. Osofsky, and H. R. Khan, "Structural and magnetic properties of nanocrystalline RuCo alloys" *Appl. Phys. Lett.* **91**, 214101 (2007).

[149] P. Riego, L. Fallarino, C. Martínez-Oliver, and A. Berger, "Magnetic anisotropy of uniaxial ferromagnets near the Curie temperature" *Phys. Rev. B* **102**, 174436 (2020).

[150] V. Pierron-Bohne, N. Ringelstein, A. Michel, S. Boukari, L. Bouzidi, N. Persat, E. Beaurepaire, M. Hehn, D. Muller, and M. C. Cadeville, "Observation of an ordered new compound $Co_{1-x}Ru_x$ prepared by MBE on a Ru buffer layer" *J. Magn. Magn. Mat.* **165**, 176 (1997).

[151] S. B. Qadri, T. M. Keller, M. Laskoski, C. A. Little, and M. S. Osofsky, "Structural and magnetic properties of nanocrystalline RuCo alloys" *Appl. Phys. Lett.* **91**, 214101 (2007).

[152] L. Fallarino, P. Riego, B. J. Kirby, C.W. Miller, and Andreas Berger, "Modulation of Magnetic Properties at the Nanometer Scale in Continuously Graded Ferromagnets" *Materials* **11**, 251 (2018).

[153] I. S. Anderson, P. J. Brown, J. M. Carpenter, G. Lander, R. Pynn, J. M. Rowe, O. Schärpf, V. F. Sears, and B. T. M. Willis, in *International Tables for Crystallography*, edited by H. Füss et al. (International Union of Crystallography, Chester, England, 2006).

[154] M. D. Kuz'min, "Shape of temperature dependence of spontaneous magnetization of ferromagnets: quantitative analysis" *Phys. Rev. Lett.* **94**, 107204 (2005).

[155] G. S. Abo, Y. K. Hong, J. Park, J. Lee, W. Lee, and B. C. Choi, "Definition of magnetic exchange length" *IEEE Trans. Magn.* **49**, 4937 (2013).

[156] E. Y. Vedmedenko, R. K. Kawakami, D. D. Sheka, P. Gambardella, A. Kirilyuk, A. Hirohata, C. Binek, O. Chubykalo-Fesenko, S. Sanvito, B. J. Kirby, J. Grollier, K. Everschor-Sitte, T. Kampfrath, C-Y. You, and A. Berger, "The 2020 magnetism roadmap" *J. Phys. D*: *Appl. Phys.* **53**, 453001 (2020).

[157] D. Erb, K. Schlage, L. Bocklage, R. Hübner, D. G. Merkel, R. Rüffer, H.-C. Wille, and R. Röhlsberger, "Disentangling magnetic order on nanostructured surfaces" *Phys. Rev. Mat.* 1, 023001(R) (2017).

[158] L. Fallarino, O. Hovorka, and A. Berger, " Field orientation dependence of magnetization reversal in thin films with perpendicular magnetic anisotropy" *Phys. Rev. B* **94**, 064408 (2016).

[159] S. Neusser and D. Grundler, "Magnonics: Spin waves on the nanoscale" *Adv. Mater.* **32**, 212927 (2009).

[160] S. Demokritov and A. Slavin, "Magnonics: From Fundamentals to Applications" *Top. Appl. Phys.* (Berlin: Springer, 2012).

[161] H. Yua, J. Xiao, and H. Schultheiss, "Magnetic texture based magnonics" arXiv:2010.09180 [physics.app-ph] (2021).

[162] G. Csaba, Á. Papp, W. Porod, "Perspectives of using spin waves for computing and signal processing" *Phys. Lett. A* **381**, 1471–1476 (2017).

[163] J. D. Joannopoulos, S. G. Johnson, J. N. Winn, and R. D. Meade, "Photonic Crystals: Molding the Flow of Light (Princeton, NJ: Princeton University Press, 2011)

[164] S. Tacchi, P. Gruszecki, M. Madami, G. Carlotti, J. W. Kłos, M. Krawczyk, A. Adeyeye, and G. Gubbiotti, *Sci. Rep.* **5**,10367 (2015).

[165] G. Gubbiotti, S. Tacchi, M. Madami, G. Carlotti, A. O. Adeyeye, and M. Kostylev, "Brillouin light scattering studies of planar metallic magnonic crystals" *J. Phys. D: Appl. Phys.* **43**, 264003 (2010).

[166] V. V. Kruglyak, S. O. Demokritov, and D. Grundler,"Magnonics" *J. Phys. D: Appl. Phys.* 43264001 (2010).

[167] S. Tacchi, G. Duerr, J. W. Klos, M. Madami, S. Neusser, G. Gubbiotti, G. Carlotti, M. Krawczyk, and D. Grundler, "Forbidden band gaps in the spin-wave spectrum of a two-dimensional bicomponent magnonic crystal" *Phys. Rev. Lett.* **109**,137202 (2012).

[168] R. A. Gallardo, A. Banholzer, K. Wagner, M. Körner, K. Lenz, M. Farle, J. Lindner, J. Fassbender, and P. Landeros," Splitting of spin-wave modes in thin films with arrays of periodic perturbations: theory and experiment" *New J. Phys.* 16, 023015 (2014).

[169] R. A. Gallardo, T. Schneider, A. Roldán-Molina, M. Langer, A. S. Núñez, K. Lenz, J. Lindner, and P. Landeros,“ Symmetry and localization properties of defect modes in magnonic superlattices” *Phys. Rev. B* 97 174404 (2018).

[170] S. Tacchi, R. E. Troncoso, M. Ahlberg, G. Gubbiotti, M. Madami, J. Åkerman, and P. Landeros, “Interfacial Dzyaloshinskii-Moriya Interaction in Pt/CoFeB Films: Effect of the Heavy-Metal Thickness” *Phys. Rev. Lett.* **118**, 147201 (2017).

[171] R. Verba, V. Tiberkevich, E. Bankowski, T. Meitzler, G. Melkov, and A. Slavin, “Conditions for the spin wave nonreciprocity in an array of dipolarly coupled magnetic nanopillars” *Appl. Phys. Lett.* **103**, 082407 (2013).

[172] G. Yu, P. Upadhyaya, Y. Fan, J. G. Alzate, W. Jiang, K. L. Wong, S. Takei, S. A. Bender, L.-T. Chang, Y. Jiang, M. Lang, J. Tang, Y. Wang, Y. Tserkovnyak, P. Khalili Amiri, and K. L. Wang, “Switching of perpendicular magnetization by spin–orbit torques in the absence of external magnetic fields”, *Nat. Nanotech.* **9**, 548–554 (2014)

[173] O. Gladii, M. Haidar, Y. Henry, M. Kostylev, and M. Bailleul, “Frequency nonreciprocity of surface spin wave in permalloy thin films” *Phys. Rev. B* **93**, 054430 (2016).

[174] K. Di, S. X. Feng, S. N. Piramanayagam, V. L. Zhang, H. S. Lim, S. C. Ng, and M. H. Kuok, “Enhancement of spin-wave nonreciprocity in magnonic crystals via synthetic antiferromagnetic coupling” *Sci. Rep.* **5**, 10153 (2015).

[175] S. Wintz, V. Tiberkevich, M. Weigand, J. Raabe, J. Lindner, A. Erbe, A. Slavin, and J. Fassbender, “Magnetic vortex cores as tunable spin-wave emitters” *Nat. Nanotech.* **11**, 948–953 (2016).

[176] R. A. Gallardo, P. Alvarado-Seguel, T. Schneider, C. Gonzalez-Fuentes, A. Roldán-Molina, K. Lenz, J. Lindner, and P. Landeros, “Spin-wave non-reciprocity in magnetization-graded ferromagnetic films” *New J. Phys.* **21**, 033026 (2019).

[177] S. S. P. Parkin, M. Hayashi, and L. Thomas, “Magnetic domain-wall racetrack memory” *Science* **320**, 197202 (2009).

[178] A. Fert, V. Cros, and J. Sampaio, “Skyrmions on the track” *Nat. Nanotechnol.* **8**, 152-156 (2013).

[179] A. Fert, N. Reyren, and V. Cros, “Magnetic Skyrmions: advances in physics and potential applications” *Nat. Rev. Mat.* **2**, 17031 (2017).